NBSIR 87-3550

Mixing in Variable Density, Isothermal Turbulent Flow and Implications for Chemically Reacting Turbulent Flows

William M. Pitts
Takashi Kashiwagi

May 1987

NBSIR 87-3550

MIXING IN VARIABLE DENSITY, ISOTHERMAL TURBULENT FLOWS AND IMPLICATIONS FOR CHEMICALLY REACTING TURBULENT FLOWS

William M. Pitts
Takashi Kashiwagi

May 1987

TABLE OF CONTENTS

LIST OF TABLES

iii

LIST OF FIGURES

Page

v

ABSTRACT

This report summarizes the research findings of a project which has been jointly funded by the Air Force Office of Scientific Research and the National Bureau of Standards. The goal of the research was to improve the fundamental understanding of chemically reacting turbulent flow. The approach which was taken was to investigate mixing in variable density flows in order to better understand the role of local density fluctuations (which result from chemical heat release) on the turbulent mixing behavior. The development of new experimental diagnostics having excellent spatial and temporal resolution is described. These techniques have been utilized to investigate a wide range of mixing properties in variable density flows. These results are summarized along with a discussion of their importance to an improved understanding of chemically reacting flow.

1. INTRODUCTION

This report summarizes the major findings of a four-year study on chemically reacting turbulent flow. This project was jointly funded by the Air Force Office of Scientific Research (contract numbers ISSA-83-00012, ISSA-84-00005, ISSA-85-00012, and ISSA-86-00008) and the National Bureau of Standards. The period covered is October 1, 1982 to September 30, 1986.

In the following sections the overall objectives of the research project are discussed, significant research accomplishments are listed and briefly described, and the significance of the findings to the understanding of chemically reacting turbulent flow is discussed.

2. PROJECT OBJECTIVES

The primary objective of this research program was the improvement of the fundamental understanding of chemically reacting turbulent flow. The most complicated aspect of this problem is the complex coupling of fluid mechanics and heat release which occurs for most flows in this class. Despite intense efforts for several decades, this complicated process has remained poorly characterized. This is unfortunate since chemically reacting turbulent flows are of paramount importance in a wide range of combustion devices and other chemical reactors which have military and industrial significance. An improved understanding of the interactions of fluid dynamics and heat release is not only necessary to improve device efficiencies and contribute to the conservation of dwindling fuel and feed stocks, but also to allow new types of designs which can limit the release of undesirable pollutants.

In order to meet the above objective an approach was chosen in which the effects of global density variations on turbulent mixing of axisymmetric jets were investigated. This path was chosen since it was felt that one of the major sources of coupling between heat release and fluid motion in a turbulent flow is through the density variations introduced by chemical heat release. In order to characterize these effects, it is first necessary to understand the effects of global density differences.

The study of mixing in variable density, turbulent flows (or any turbulent flow for that matter) is complicated by the wide range of spatial and temporal scales which are of importance. These scales vary from the full dimensions of the flow field down to the smallest scales where turbulent dissipation occurs. It is clear that in order to obtain an improved characterization of these processes diagnostics having high spatial and

2

temporal resolution are required. Since suitable diagnostics were not available, an important secondary goal for the project became the development of new experimental techniques for the study of concentration and velocity fluctuations in variable density flows. The importance of large scale turbulent structures in these flows fields necessitated the development of multi-point diagnostics capable of high temporal and spatial resolution. A digital line camera was designed and a prototype constructed. Preliminary experiments utilizing the camera have been encouraging and development is continuing.

3. RESEARCH ACCOMPLISHMENTS

In the subsection which follows, the development of new diagnostics are described. The findings of an extensive study of mixing in variable density turbulent flows are then summarized. Work in this laboratory, as well as elsewhere, has demonstrated the importance of these findings to an improved understanding of chemically reacting turbulent flow. This point is discussed in the last subsection.

3.1 DIAGNOSTIC DEVELOPMENT

Throughout the course of this project there was an emphasis on the acquisition of real-time data having high spatial resolution and accuracy. Very few suitable experimental techniques were available and a great deal of effort was directed toward the development of unique capabilities for the measurement of concentration and velocity in variable density flow fields. Significant progress has been made on the development of the necessary diagnostic tools.

3.1.1 Concentration Measurement Using Rayleigh Light Scattering

The development of Rayleigh light scattering as a real-time diagnostic of concentration fluctuations within small spatial volumes of turbulent binary gas mixtures was completed during the very early stages of the project period. Building on earlier work [1,2] it was demonstrated [3,4] that Rayleigh light scattering can be utilized to measure a wide range of properties in these flow fields.

The intensity of light scattered by a gas is proportional to the Rayleigh scattering cross section. This scattering cross section is in turn related to the index of refraction of the gas. Since the refractive indices of individual gases vary, scattering intensity varies from gas to gas. For mixtures, the scattering cross sections for the different gases are additive. A measurement of scattering intensity from a binary gas mixture, following calibration in the pure components, allows the concentrations of the two gases in the observation volume to be determined.

Figure 1 shows the experimental apparatus which was developed for Rayleigh light scattering measurements. In order to test this system, real-time concentration data were recorded in the turbulent flow field formed by an axisymmetric jet of methane (Re = 4130) flowing into a slow coflow of air. It was demonstrated [3,4] that this system is capable of recording real-time measurements of methane concentration at data rates as high as 10 kHz for observation volumes as small as 0.0003 mm^3 . The accuracy of individual measurements was estimated to be $\approx$ 1.9% at the highest data rate.

From the resulting real-time data records such flow properties as the time-averaged concentration, root mean square (RMS) in the concentration fluctuations, and the concentration skewness and kurtosis were calculated.

4

Figure 2 shows the behavior of the time-averaged methane concentration in the radial direction for a downstream distance of 30 r_o. By using fast Fourier transform analysis it was also possible to calculate the frequency spectrum and correlation functions for the concentration fluctuations.

The availability of real-time data allowed a determination of whether or not jet fluid was present in the imaged volume during the observation time. In this manner, the intermittency function (based on the presence or absence of jet fluid) could be determined and then utilized to provide conditionally-sampled measurements for the properties described above.

Even though the results [3,4] of this work were of a preliminary nature, they represented the most extensive and complete set of data for a variable density flow available in the literature at the time of their publication. Where comparisons were possible, results [3,4] were found to be in excellent agreement with measurements reported in the literature.

3.1.2 Simultaneous Concentration and Velocity Measurement

The development of the Rayleigh light scattering technique provided a powerful means for monitoring concentration behavior in a turbulent flow field of two gases. However, in order to more fully characterize turbulent behavior in variable density flows, measurements for velocity are also required. Of particular importance is the capability for simultaneous measurements of concentration and velocity which allows such parameters as the cross-correlation coefficient (R_{uc}) of velocity and concentration to be calculated. Such correlations are very important since they often appear in models which attempt to provide closure for the Navier-Stokes equations and in treatments which utilize Favre averaging [5]. Such measurements have been very difficult

5

to make in the past and very few comparisons between theoretical estimates and experimental findings are available.

Either of two techniques, hot-wire anemometry (HWA) and laser Doppler velocimetry (LDV), are usually employed for real-time velocity measurement. LDV requires seeding of the flow with particles. This results in a strong Mie scattering which completely obscures the Rayleigh light scattering signal necessary for concentration measurement. Even though experiments have demonstrated that simultaneous measurements of concentration and velocity are possible in lightly seeded flows [6], it has not been possible to make real-time measurements. For this reason, HWA was chosen as the velocity diagnostic.

HWA in variable density flows is complicated by the variations in molecular thermal conductivity which occur as the composition of the gases around the probe changes. As a result, the response of the HWA is not only sensitive to velocity changes, but also to concentration variations. This sensitivity has been used as the basis for probes designed to measure concentration in binary gas mixtures [7]. By combining two probes having different heat transfer properties it has also been possible to make simultaneous measurements of concentration and velocity [8,9]. However, these measurements require extensive calibrations and data manipulation and have not come into widespread or routine use.

By combining the HWA and Rayleigh light scattering techniques it is possible to mitigate some of the limitations of HWA for velocity measurements in variable density flow fields consisting of two gases. The Rayleigh light scattering technique provides real-time concentration measurements which can be utilized to correct the response of the HWA for variations in gas

6

composition once the velocity probe has been calibrated in a series of mixtures. The necessary calibrations are considerably simpler than those required when two hot-wires are employed. Limitations of such an approach include the need for an obtrusive probe and the necessity of physically separating the observation volume for the Rayleigh light scattering and the position of the hot-wire (to avoid scattering).

Experimental work [10] has shown that the limitations mentioned above are not serious and that the combination of Rayleigh light scattering and HWA can be utilized for accurate, real-time measurement of concentration and velocity in variable density flows. Figure 3 shows an example of the real-time behavior of concentration and velocity for a turbulent jet of propane flowing into a coflow of air. Such data records were utilized to calculate time-averages, rms values, and cross-correlation values for the velocity and concentration fluctuations of propane and methane jets. In all cases the experimental measurements were in excellent agreement [10] with the limited data available in the literature.

The measurements reported in [10] are for a single hot-wire (or hot-film) aligned so that the probe is sensitive to velocity in the axial direction of the jet flows. It is possible to also utilize an "X-probe" consisting of two wires oriented at 45° in order to measure both the axial and radial components of velocity. During the past year the response of such a probe to variable density flows as well as the effects of flow direction have been extensively investigated. In the near future this X-probe will be combined with the Rayleigh light scattering system in order to form an experimental system which can make real-time measurements of concentration and two components of velocity in variable density flow fields. This system will be capable of

7

characterizing variable density turbulent flow fields to a degree which has heretofore been impossible.

As part of the calibration work necessary to employ these HWA probes, various correlations available in the literature for the heat loss from a cylinder were considered. It was discovered that none of these correlations were successful in correlating an extensive series of calibrations performed in ten different gases [11,12]. The most widely quoted correlation for different gases utilized a correction based on the Prandtl number (Pr) to correct for variations in molecular properties [13-15]. This correlation was found to be unsatisfactory for the gases investigated during this study. Extensive analysis [11,12] of the data showed that it is necessary to consider the temperature dependence of the molecular properties in order to obtain accurate correlations. Figure 4 is a plot of the heat transfer behavior (in terms of the nondimensional Nusselt number) as a function of flow velocity (in terms of the nondimensional Reynolds number based on the probe diameter). The correlation of the results for the nine gases shown is excellent.

Other heat transfer characteristics such as thermal slip and surface accommodation were also investigated during the course of this study [11,12]. In particular, it was shown that the heat transfer from a cylinder to helium is strongly influenced by surface accommodation. Using theories previously developed for treating this process [16] it was possible to correct the measurements for this effect and obtain an accurate correlation of the heat transfer behavior of helium with the results for other gases. The helium data included in figure 4 have been analyzed in this manner. The measurements also yielded an vastly improved understanding of the dependence of the heat

8

transfer process on Re and transitions in flow behavior which occur as the Re is varied.

The manuscripts which resulted from this work [10,11,12] are not only significant for their importance to researchers who wish to utilize HWA in different gases, but are also important for the much wider field of heat transfer. The results considerably modify current concepts concerning the role of molecular properties in heat transfer behavior.

Extensive measurements [17] have also been made for mixtures of gases. For these mixtures the procedure described above does not provide accurate correlations for the heat transfer measurements. Systematic variations are observed with the mole fractions of the components which have tentatively been ascribed to the effects of thermal diffusion on the heat transfer behavior. If thermal diffusion is indeed the source of the variations, it is required that its effects on heat transfer be roughly ten times larger than reported in the literature. Dr. Howard Baum is currently developing a theory [17] for this process which is designed to allow a test of this hypothesis.

3.1.3 Development of a Digital Line Camera for Concentration Measurement

The flow diagnostic techniques described above are designed to allow accurate point measurements of velocity and concentration. Measurements utilizing these techniques as well as findings in other laboratories have suggested the importance of large scale structures for mixing in turbulent flows such as axisymmetric jets. The availability of real-time point measurements allows some characterization of these structures through the determination of intermittency functions and conditional sampling. However, such measurements provide very limited information about individual structures

9

and their role in the entrainment of surrounding gases. Clearly, simultaneous measurements at many different points in space would provide much more information concerning the structure and role of these large scale structures in the turbulent mixing process.

Recently there has been a great deal of research activity (e.g., [18-23]) on the development of optical diagnostics which are capable of nonobtrusive, multi-point measurements in flow fields. Such imaging experiments have been reported along lines [18], in planes [19-21], and in three dimensions [23]. A wide range of optical processes such as Rayleigh [19,23], Raman [20], Mie scattering [19] and fluorescence [18,21,22] have been employed. Even though there are exceptions, most of these experiments are characterized by the need for image intensification (due to the relative insensitivity of the solid-state detectors which are usually employed) and the use of high-powered lasers which provide sufficient signal levels to allow the optical measurements, but which limit the experiments to low repetition rates.

Due to the ability of imaging experiments to provide a more complete characterization of large scale structures in turbulent flows, it was clear that a system utilizing Rayleigh light scattering for quantitative mass fraction measurement would be very useful. A short proposal was prepared and the necessary funding for the development of a digital line camera system was provided internally by the National Bureau of Standards. Note that a similar unintensified system has been utilized for concentration measurements in a water jet [22].

A set of design goals were developed for the camera. The most important of these are listed here:

1. A spatial resolution of 400 μm along the line.

10

2. Line readout rates greater than a kHz.

3. Concentration measurements having an absolute accuracy of a few percent.

4. Utilization of an existing CW Ar ion laser and data acquisition system.

5. Use of commercially-available components.

The first three of these goals were chosen to be consistent with the capabilities of our experimental system for single point measurements of concentration. The last two were required to minimize the cost of the system and simplify its design and construction. These criteria were found to be in competition with one another and it was necessary to make compromises in the design of the camera.

An analysis [24] of the intensity of scattered light from the Ar$^+$ ion laser beam and the sensitivity of commercially available solid-state line detectors indicated that image intensification would be required in order for the line camera to operate at the required data rates. This requirement turned out to be the most difficult technical challenge of the camera design.

There are two major types of image intensifiers available commercially. These are known as generation I (gen I) and generation II (gen II). Gen I tubes consist of a photocathode, accelerating and focusing electronics for electrons emitted by the photocathode, and a phosphor screen. The optical gain of the device results from the fact that a single accelerated electron striking the phosphor screen results in the production of many photons.

Gen II tubes are similar to gen I tubes with the exception that a microchannel plate (MCP) is inserted between the photocathode and the phosphor screen. The MCP is an active device which can produce electron gains of

10^3-10^4. Since the channels which form the MCP are aligned, any electron "image" present on the input face is maintained at the other end of the MCP.

Electrons emitted by the photocathode of a gen II image intensifier are focused (either by proximity or electrically) onto the MCP and the resulting amplified electron image from the MCP is focused onto a photocathode. Since the MCP provides a very high gain, a single gen II image intensifier has a much higher light gain than a single gen I tube. It is necessary to cascade two or three gen I tubes in order to obtain intensification comparable to a single gen II tube.

In most flow imaging experiments reported thus far gen II tubes have been utilized. However we discovered [24] that for real-time imaging there is a serious problem due to the maximum light output which can be generated by this type of image intensifier. This limitation results from the limited output current of the individual channels of the MCP. Calculations indicated that the maximum brightness which can be generated by a gen II tube is comparable to that available from the Rayleigh light scattering experiment and is not sufficient for real-time detection using commercial, solid-state line detectors. Since only moderate light gains were necessary, a gen I tube was chosen as the image intensifier. These tubes can operate at much higher current levels than the second generation devices and can therefore produce more intense light outputs.

Measurements at data rates greater than a kHz also require consideration of the response time of the phosphor screen used in the intensifier. The P-20 phosphor employed for standard tubes has a long-lived tail in its temporal decay and for this reason is unsuitable for this application. A P-47 phosphor screen was chosen instead. This screen has a submicrosecond lifetime, but it

12

is less efficient than P-20 and the overall gain of a single stage is significantly reduced. The final selection for the image intensifier consisted of two stages of gen I tubes equipped with P-47 phosphor screens.

The detector chosen for the camera was a Reticon RL128S* line detector which consists of 128 pixels on 25 μm centers. A 4:1 reduction fiber optic taper was utilized to couple the detector and the image intensifier. The camera was completed by the addition of a f/1.9 1:1 focusing lens for imaging the scattered light onto the image intensifier. With this arrangement each pixel corresponds to a 100 μm length of the image so that the entire line image covers 12.8 mm. Figure 5 shows a schematic for the prototype camera.

The line detector is equipped with electronics which generate voltages that are proportional to the light detected during the integration period on an individual pixel. The voltages for the 128 pixels appear sequentially on the output. These voltages are digitized and stored in the memory of a minicomputer. Since the maximum data rate for the acquisition system used is 333 kHz, the maximum line read-out rate is limited to 2.2 kHz. Figure 6 shows the overall system for line measurements of concentration including the digital line camera, the flow system, and the Ar^+ ion laser.

In order to test the system, line measurements of propane mole fraction for a propane jet flowing into a slow coflow of air have been recorded. Figure 7 shows an example of the concentration behavior across the radial profile of the jet at a downstream distance of 5 jet diameters and a line read-out rate of 837 Hz. The total data acquisition time was $\approx$ 300 ms. Even

---

*Certain commercial equipment, instruments, or materials are identified in this paper in order to adequately specify the experimental procedure. Such identification does not imply recommendation or endorsement by the National Bureau of Standards nor does it imply the instruments or equipment are necessarily the best available for the purpose.

13

though the time resolution is not sufficient to fully resolve small details, the importance of large scale structures is clear. The results of such measurements can be time-averaged to yield the contour of the radial profile. Figure 8 shows the results for five downstream positions. The growth and spread of the turbulent boundary layers is evident.

While the performance of the initial camera prototype has been very encouraging, it has not been possible to reach the full time resolution potential of the camera due to limitations in the gain of the image intensifier. A new, three-stage tube has been ordered and will be installed shortly. This gen I image intensifier will provide a higher gain due to the additional stage of amplification. It is also equipped with P-46 phosphor screens which have the same short lifetime properties of P-47, but which have outputs at longer wavelengths (green). Green light is more efficiently transmitted by the fiber optic taper and detected more efficiently by the line scanner. This modification should therefore increase the sensitivity of the tube significantly.

3.2 CHARACTERIZATION OF MIXING AND VELOCITY BEHAVIOR IN AXISYMMETRIC JETS

3.2.1 Mixing in a Turbulent, Axisymmetric Jet of Methane

As part of the development of Rayleigh light scattering as a diagnostic for concentration, extensive measurements of such flow properties as time-averaged concentration, unmixedness, skewness, kurtosis, concentration fluctuation spectra, and correlation functions were made [3,4]. The existence of time-resolved data records also allowed the intermittency functions for the flow field to be determined and from these it was possible to generate conditionally-averaged measurements of these flow properties.

14

Data were recorded at various positions along the jet centerline and across the radial profile of the jet for one downstream position ($z/r_o = 35$). In all cases where literature sources were available for comparison there was excellent agreement. The availability of real-time data allowed the existence of large-scale ramp-like structures in the intermittent region of the flow field to be identified. Such structures are believed [25,26] to be the primary mechanism by which jet entrainment occurs and for this reason their characterization is crucial.

Even though the findings of the study [3,4] were of a preliminary nature, they were chosen for comparison purposes with conserved scalar measurements in a hydrogen jet flame [27,28]. These authors felt the measurements were the most complete and accurate available at the time. A remarkable similarity was found between mixing in the isothermal and combusting flows. The significance of this finding is discussed below.

3.2.2 Simultaneous Measurements of Concentration and Velocity in a Propane Jet

As a test of the combined hot-probe anemometry and Rayleigh light scattering diagnostic, real-time concentration and velocity data were recorded in jet flows of propane entering a slow coflow of air [10]. Preliminary measurements which were recorded are significant due to the limited number of such measurements which have been reported in the literature for variable density flows. For instance, time-averaged measurements of centerline velocity showed that the data could be fit in the form

$$U_o/\overline{U}_c = K_u (z - z_o)/r_\epsilon \tag{1}$$

15

where r_ϵ is the effective radius defined as $(\rho_o/\rho_\infty)^{1/2}r_o$. A least squares fit of the results gave $K_u = 0.082$ which is close to the value of 0.081 recommended by both List [29] and Chen and Rodi [30]. Values of the correlation coefficients for velocity and concentration were also calculated as a function of downstream position. Literature comparisons were very scare, but measurements by Antonia et al. [31], Chevray and Tutu [32], and Catalano et al. [33] showed that values of R_{uc} measured in this study were consistent with previous measurements. The findings suggest that R_{uc} grows to an asymptotic value of ≈ 0.39 on the jet centerline in this variable density flow.

3.2.3 Density and Reynolds Number Effects on Mixing in Axisymmetric Jets

An extensive study [34] of the effects of density and Reynolds number variations on mixing in turbulent axisymmetric jets was performed. Qualitative information concerning the flows was obtained using time-resolved shadowgraphs while Rayleigh light scattering was utilized to investigate quantitatively the centerline mixing behavior. Table 1 lists the gas pairs investigated in this study, the ratio of jet to coflow densities, Re based on the jet diameter, and whether or not shadowgraph and Rayleigh data were taken.

Figure 9 shows the experimental arrangement used to record shadowgraphs of the variable density jet flows. The diameter of the shadowgraphs is 76 mm and the light pulse has a measured FWHM of 165 μs with a total duration of 310 μs. It must be remembered that shadowgraphs provide an integrated view of the flow field and that the signal is proportional to the second derivative of the index of refraction variations which occur along the path of the light beam.

16

For these reasons, extreme caution must be utilized in drawing conclusions from such photographs. However, with this in mind, it is possible to characterize some of the effects of density and Reynolds number variations on jet mixing behavior from the series of shadowgraphs which have been recorded.

Figure 10 provides a dramatic example of the effects of density differences on the mixing behavior of a turbulent jet. Shadowgraph are shown for a jet flow of sulfur hexafluoride into air with Re = 3950. The initial jet density is 5.1 times higher than that of the surrounding air. As is clearly shown by the shadowgraph covering the downstream region from $z/r_o = 25$ to 45 , the initial momentum of the jet is not high enough to overcome the negative buoyancy (the jet is orientated vertically) of the flow and the jet forms a fountain with jet fluid falling back through the surrounding coflow. Interestingly, as can be seen in figure 11, this effect disappears for Re of 7890 and 11860.

Shadowgraphs for flows covering jet to coflow density ratios of 0.14 to 5.1 are shown in figure 12. The following conclusions have been drawn concerning the effects of density and Re differences on mixing in these flows from these and other shadowgraphs.

  1. The initial density ratio effects the shape of the vortices at
      downstream positions in the flow field. Increasing density ratios
      result in lengthening of vortices in the axial direction.

  2. Changes in the density ratio effect the initial development of
      turbulence in the jets. For smaller values of ρ_o/ρ_∞ the flow
      distance required for initial growth of vortices is shorter.

Figure 13 shows shadowgraphs recorded for jet flows of propane into air at three different Re. From these photographs as well as those shown in figure 11, the general effects of changes in Re can be summarized as

  1. As the Re is increased the turbulent structures in the flow field
      extend to smaller scales.

17

2. Increasing the Re has very little effect on the angle of spread for a given gas pair.

3. Turbulent structures develop at shorter flow distances as the Re is increased.

Even though the shadowgraphs provided qualitative information concerning mixing in variable density turbulent flows, very little quantitative information could be obtained. Rayleigh light scattering was utilized to perform quantitative measurements of fluid concentration behavior along the centerlines of the jets.

Time-averaged concentration measurements provide an excellent example of how significantly density differences can modify mixing. Figure 14 shows experimental values of inverse time-averaged mass fraction ($1/\overline{Y}_m$) plotted as a function of nondimensionalized downstream position for different jets having a wide range of density ratio. The data fall on straight lines having slopes which decrease with increasing density ratio and virtual origins (value of z where $1/\overline{Y}_m$ extrapolates to zero) which move upstream as the density ratio increases.

In the early 1950's Thring and Newby [35] suggested that the centerline mixing behavior of axisymmetric turbulent jets could be correlated using an expression which can be written as

$$1/\overline{Y}_m = K_c z/r_\epsilon + (\rho_\omega/\rho_o - 1)K'$$ (2)

where r_ϵ is the effective radius defined earlier and K_c and K' are constants which are determined by radial integrations of velocity and concentration across the flow field. This equation can be derived utilizing conservation equations and assuming self-similarity. It is strictly valid only for downstream positions where $\overline{\rho}_m \approx \rho_o$.

18

The predicted behavior of plots of $1/\overline{Y}_m$ versus z/r_o using eq (2) are shown in figure 15 for $K_c = 0.114$ and $K' = 0.5$. Comparison with the experimental results in figure 14 shows that there is excellent agreement. The dependence of the slopes of the plots on ρ_o/ρ_∞ has been documented in the literature previously (e.g., [36,37]), but to our knowledge, this is the first time that the predicted dependence of z_o on the this parameter has been confirmed.

Similar data were recorded for axisymmetric jets in which the Reynolds number was varied. These measurements showed that the principal effect of increasing the Re was to shift the virtual origin, z_o, downstream. Slopes of plots of $1/\overline{Y}_m$ versus z/r_o were independent of Re. This suggests that the centerline mixing behavior in these flow fields is due primarily to large scale turbulent structures which should be independent of Re (i.e., inviscid flow).

The availability of time-resolved measurements allowed the behavior of centerline unmixedness (defined as the RMS of the concentration fluctuations, Y'_m, divided by $\overline{Y}_m$) to be determined as a function of ρ_o/ρ_∞ and Re. Figure 16 is a plot of $Y'_m/\overline{Y}_m$ versus z/r_o for six variable density flows. It is clear that in each case unmixedness values are approaching a common asymptote of $\approx$ 0.23, but that the flow distance required to attain this value is strongly dependent on ρ_o/ρ_∞ with higher ratio flows requiring longer flow distances. There are very few measurements or theoretical predictions of unmixedness in variable density flows reported in the literature. This study was the first to provide data for a wide range of ρ_o/ρ_∞.

In order to gain some understanding of the role of density ratio on the flow distance required to attain the unmixedness asymptote, the experimental

19

values of $Y'_m/\overline{Y}_m$ were replotted as a function of z/r_ϵ as shown in figure 17.
It is clear that plotting the data in this manner results in a collapse of the
growth curves for unmixedness and that r_ϵ serves as a scaling parameter for
the growth. This conclusion is surprising in that the unmixedness development
is occurring in a flow region where the condition $\overline{\rho}_m \approx \rho_o$ is not met and the
development which leads to the definition of r_ϵ is not strictly valid. At the
same time it does suggest that r_ϵ is a true scaling parameter which not only
results in a collapse of time-averaged data, but also scales the development
of turbulent structure in the flow field.

Similar measurements in C_3H_8/air (see fig. 18) and SF_6/air flows have
shown that the asymptotic value of unmixedness is independent of Re, but that
the flow distance required to attain the asymptote increases as the Re is
increased. The longer flow distances required for turbulence growth in the
higher Re flows results in the downstream shifts of the virtual origins
observed for plots of $1/\overline{Y}_m$ as functions of z/r_o. The observed Re dependence
of the flow distance required to attain fully-developed flow was surprising
since fully-developed turbulent behavior is generally associated with high Re.
The independence of the asymptotic value of $Y'_m/\overline{Y}_m$ on Re once again highlights
the importance of large scale structures in turbulent mixing behavior.

It was hypothesized [34] that the longer flow distances required for
fully-developed flow at higher Re is connected with development of smaller
scale vortices in the flow fields at higher Re. If a "pseudo-equilibrium"
exists between the different vortical scales, a longer flow distance would be
required for the entire turbulent structure to come into equilibrium at the
higher Re. More sophisticated experiments will be necessary to test this
hypothesis. Whether or not this hypothesis is correct, a more complete

20

characterization of the growth of centerline unmixedness in these flows is required so that parameters which control the growth of turbulence in flow fields can be identified.

The time records were also used to calculate skewness (third moment) and kurtosis values (fourth moment) for concentration fluctuations. Distinct effects of density ratio were observed on the centerline behavior of these parameters, but in the absence of theoretical guidance it was not possible to relate these variations to physical modifications of the mixing behavior.

The manuscript which was written to describe these results [34] contains extensive comparison with previous literature findings. Generally, quantitative agreement is excellent. Possible sources of disagreement, such as the effects of buoyancy and the use of a coflow, were also analyzed and were generally found to be minor perturbations. It was concluded that the results are indicative of mixing behavior in free axisymmetric jets. The use of a wide range of density ratios and Re resulted in the identification of dependencies in the mixing behavior which had not been reported previously.

4. IMPORTANCE OF ISOTHERMAL STUDIES TO AN IMPROVED UNDERSTANDING OF TURBULENT REACTING FLOWS

The significance of findings from the isothermal flow studies for improving the understanding of the more complicated case of chemically reacting flows was considered where appropriate. These analyses resulted in a more clearly defined perception of the role of density variations (both global and local) in chemically reacting turbulent flows. Consideration of mixing behavior in the isothermal mixing regions of lifted and blown out turbulent jet diffusion flames resulted in new correlation procedures for describing these stabilization characteristics and suggested new physical models to

21

understand the behaviors. The role of local Re variations on mixing in chemically reacting turbulent flows has been assessed. These points are discussed in this section.

4.1 Similarity of Mixing in Isothermal and Reacting Flows

Numerical data from the original Rayleigh light scattering study of methane [3,4] were provided to investigators at General Electric Corporate Research and Development Center for comparison with extensive experimental measurements recorded for a turbulent hydrogen jet flames. Drake et al. [27,28] found that radial profiles of the first four moments of concentration fluctuations (time-average, RMS, skewness, and kurtosis) for the isothermal and reacting flow (in terms of the conserved scalar concentration, ζ [38]) were very similar. Such agreement suggests that heat release and combustion have very little effect on the probability distribution functions (PDF) of scalar mixing in turbulent reacting flows. This conclusion is extremely important because it implies that the results of isothermal mixing studies can be applied directly to chemically reacting turbulent flows and thus provides additional justification for the approach taken in our own study. Theorists have long used isothermal mixing results as the basis for models of chemically reacting turbulent flow [39].

Drake et al. [27,28] also utilized the isothermal results of our earlier study along with their own findings to test a parametric expression developed by Effelsberg and Peters [40] which divided the conserved scalar PDF into nonturbulent, fully turbulent, and superlayer parts. These authors concluded that the measurements were not consistent with this model since the results required that more than 50% of the PDF be due to superlayer contributions. An

22

alternate interpretation was offered in which the "apparent" superlayer was attributed to the presence of large scale "ramp-like" structures in the flow field. Such structures have been observed in time records recorded in our earlier work [3,4] and by other researchers (e.g., [31,41,42]).

4.2 Lift-off and Blow-Out of Turbulent Jet Diffusion Flames

There are certain properties of combusting jets for which isothermal findings are directly applicable. In particular, lift-off and blow out of turbulent jet diffusion flames must depend on the concentration and velocity behavior of the turbulent flow upstream of the region where combustion or blow out occurs. The results of our isothermal studies as well as other findings available in the literature have been utilized [54] to develop a procedure which is capable of accurately predicting experimental lift-off heights as a function of jet exit velocity and blow out velocities as a function of jet diameter for turbulent jet diffusion flames of many different fuels. Interestingly, only time-averaged properties have been considered and it has not been necessary to consider the actual turbulent behavior of the flow. This is significant since most theoretical treatments either assume flame stability is due to an equilibrium of flow velocities and turbulent flame speeds (which depend on small scale turbulent structure) [43-47] or to flame extinction processes in small scale structures [48-51].

A radically different explanation for flame stability has been suggested by Broadwell et al. [52]. These researchers have argued that flame stability is determined by the reentrainment of hot combustion gases (expelled by the passage of earlier large scale structures) by large scale structures in the flow field. These gases are rapidly mixed with the jet gases and if the

turbulent mixing time, τ_d is longer than the chemical ignition time, τ_c, of the fuel/air mixture in the jet, the structure will be ignited and the combustion stabilized. When the mixing time becomes shorter than the chemical reaction time ($\tau_c > \tau_d$) combustion can no longer be sustained.

The impetus for our investigation of flame stability mechanism was the extensive experimental investigations of lift-off [47] and blow out [53] of turbulent jet flames by Kalghatgi. He found that his results for lift-off heights as a function of velocity for different fuels were well correlated by an expression which can be approximated as

$$h = C_h (U_o/(S_b)^2_{max})\nu_o (\rho_o/\rho_\infty)^{1.5}, \tag{3}$$

where C_h is a constant, $(S_b)_{max}$ is the maximum laminar flame speed for the fuel and air, and the density term is an approximation for a more complicated expression. The form of this equation was based on dimensional analysis. The inclusion of ν_o in the expression reflects the important role small scale turbulent structures are believed to play in this stability behavior.

Blow out velocities as a function of jet diameter were found to have a similar dependence on density and ν_o [53]. This correlation can be written as

$$(U_o)_b = C_b r_\epsilon (S_b)^2_{max}/(Y_s \nu_o (\rho_o/\rho_\infty)^{1.5}), \tag{4}$$

where C_b is a constant and Y_s is the mass fraction of fuel in a stoichiometric mixture with air.

Attempts to predict the exponent of 1.5 for the density ratios in eqs (3) and (4) in terms of the known concentration and velocity fields of isothermal, variable density turbulent jets were not successful. On the other hand, correlations in which the term $\nu_o (\rho_o/\rho_\infty)^{1.5}$ were omitted from eqs (3) and (4)

24

were found to accurately correlate Kalghatgi's experimental findings. The simplicity of these correlations suggested that the time-averaged properties of the flow field might be employed to predict lift-off heights and blow out velocities. Subsequent calculations [54] have shown this to be the case.

The first step in the procedure is to calculate the time-averaged mass fraction contour in the flow field along which the laminar flame speed is a maximum. Both theory [43-45] and measurements [44,45,55] in turbulent jet flames have shown that the most probable location for the shortest distance between the nozzle and the instantaneous flame position is along this contour. Figure 19 shows the form of this contour for an ethylene jet. In order to make these calculations, the centerline mixing behavior is taken from our variable density study and the radial behavior is based on expressions given in Chen and Rodi's book [30]. Shifts in virtual origin with density ratio and Re have been ignored.

An empirical procedure was then utilized to derive an expression for the local velocity (U_l) along the contour which results in the proper dependencies [47] of lift-off heights on jet diameter (nearly independent) and exit velocity (linearly dependent). The resulting expression has the form

$$U_l = C_h'' z^2 (S_b)_{max}^2 Y_l^2 / r_\epsilon \tag{5}$$

where Y_l is the mass fraction of fuel necessary for $(S_b)_{max}$. The corresponding velocity at the jet exit is then calculated utilizing the known axial and radial dependencies for velocity [30]. C_h'' is a constant parameter which has the units of an inverse kinematic viscosity. In order to determine C_h'' a single experimental measurement of h for ethylene from the turbulent jet

25

flame data of Kalghatgi [47] was utilized. A value of $C_h'' = 0.0484$ s/cm^2 resulted.

This calculational procedure was utilized to calculate values of the lift-off height as a function of exit velocity for different fuels. Figure 20 reproduces the results of the calculation [54] for fuel jets of methane, ethylene, and propane and compares the predictions with the experimental results of Kalghatgi [47]. The agreement is excellent.

The success of the calculational procedure in reproducing the experimental findings for lift-off heights of turbulent jet diffusion flames suggests that small scale vortices may not be important in flame stability since only global mixing properties which are independent of Re have been utilized. The role of small scale structures cannot be total discounted since it is possible that their properties may be correlated with the variables included in eq (5) in some manner. The fluctuation properties of the concentration and velocity in the radial positions where these calculations have been made are not well enough characterized to test this.

The form of eq (5) is consistent with the model for turbulent combustion suggested by Broadwell et al. [52] in which flame stability is determined by the behavior of large scale turbulent structures. However, it should be noted that the authors reported, but did not test, an expression for lift-off heights which is not consistent with the experimental observations of Kalghatgi [47]. If their model is correct, eq. (5) suggests that the chemical reaction time is inversely proportional to $(S_b)_{max}^2$ and that the turbulent mixing time is proportional to z^2/r_ϵ. The latter proportionality suggests that two lengths scales are necessary to characterize the mixing time; one which increases as z/r_ϵ and a second which scales as z. It has already been

26

shown that z/r_ϵ is the proper nondimensionalizing length scale for centerline mixing. Previous studies [30,36] have concluded that the radial spreading rate as a function of downstream distance is linearly dependent on z and independent of density ratio. It is therefore expected that r_d will scale with the product of z and z/r_ϵ.

The appearance of the Y_1^2 in eq (5) is at first perplexing. Calculations have shown that it serves to make the calculated values of U_o independent of Y_1. This is consistent with the absence of this parameter in the correlation shown in figure 20 and suggests that r_d may be independent of radial position in these flows.

It was possible to extend this calculational procedure to the prediction of blow out velocities [54]. It is known [44,45,53] that blow out occurs in these flames well before the contour represented in figure 19 reaches the jet centerline. This suggests that flame extinction occurs when

$$U_1 > U_b, \qquad (6)$$

where U_b is a well-defined velocity. In order to reproduce the experimental finding of Kalghatgi [53] for $(U_o)_b$ as functions of jet radius and fuel it is necessary that

$$U_b = C_b (S_b)_{max}^2 r_o. \qquad (7)$$

A value of $C_b = 1.5$ s/cm^2 was determined using one of Kalghtgi's experimental measurements [53]. Figure 21 compares predicted blow out behaviors (solid lines) with Kalghatgi's experimental results for five fuels. The agreement is outstanding.

27

Broadwell et al. [52] showed that their hypothesis concerning the role of large scale structures in the stability of turbulent jet diffusion flames led to an expression which also accurately correlated Kalghatgi's [53] blow out data. Equation (7) is very similar to their development with the exception that it is based on the local flow velocity while Broadwell et al. [52] found it necessary to assume that flame extinction occurred when the centerline mass fraction fell to some constant percentage of the value for stoichiometric burning. The similarity of the two expressions lends support to their flame stability theory.

4.3 Application of Isothermal Findings to Turbulent Mixing in Combusting Regions of Turbulent Jet Flames

The similarity of the isothermal measurements of turbulent structure [3,4] and those made in a hydrogen/air diffusion flame [27,28] suggests that the combustion process may not significantly alter turbulent mixing behavior. If this is the case, it is expected that the principal effect of combustion on turbulent mixing arises from the density variations induced by heat release.

In an earlier manuscript [54] the role of these density fluctuations on mixing in turbulent jet flames has been discussed. Several particular cases were identified for which these density variations might be expected to approximate those in isothermal flows having global density variations. As summarized here, experimental findings suggest this approach may have some validity in certain downstream positions of combusting flow fields.

Figure 22 is a representation of radial density profiles in turbulent jet flames of hydrogen and a typical hydrocarbon (methane). One of the interesting aspects of the hydrogen jet flame is that the heated products and the cold fuel have very nearly the same densities. In the near field of the

jet, combustion occurs primarily in the outer regions of the flow so that the density is constant over nearly the full radial range of the turbulent flow. For this reason, the mixing behavior of the flow near the jet exit should be very similar to that observed for a constant density, isothermal flow. Experimental evidence supporting or contradicting this conclusion was not available in the literature.

Similar arguments lead to a different conclusion for the near-field mixing behavior in hydrocarbon turbulent jet diffusion flames. Since the heated combustion products are much less dense than the cold fuel, in the near field the flow consists of a dense inner turbulent jet flowing into considerably less dense surroundings (see fig. 22). This view is supported by shadowgraphs recorded by Wohl et al. [56] and by the recent schlieren study of Savas and Gollahalli [57] which show a more dense turbulent fuel jet entering an apparently laminar, less dense surroundings.

Several groups (e.g., [58] and [59]) have recorded concentration measurements in the near fields of both isothermal and combusting jets of hydrocarbon fuel gases. In general, the flame jets have longer potential cores, develop turbulent behavior further downstream, and have centerline fuel mass fractions which fall off less rapidly with downstream distance than in the corresponding isothermal flows. Based on the isothermal findings discussed above, these behaviors are exactly those expected for a dense jet flowing into less dense surroundings.

As the combusting jet move further downstream the most likely position for combustion moves closer to the centerline and the radial density profiles are modified. In the case of the hydrogen flame the result is that the central part of radial profile has a density which remains nearly constant,

29

but in the outer regions of the flow there is a rapid increase in density (see fig. 22, $z/r_o = 80$). The condition necessary for the application of the isothermal findings (namely, $\overline{\rho}_m \approx \rho_\infty$) is not fulfilled and it is not expected that the centerline decay will obey a relation having the form of eq (2).

Detailed measurements of conserved scalar concentrations in turbulent jet flames of hydrogen are available [60,61]. In general, the authors have not analyzed their data in the form suggested by eq (2), but it appears that the centerline decay of conserved hydrogen concentration does not have a hyperbolic fall off with increasing downstream distance.

In the case of hydrocarbon fuels Hans Kremer (as described by Ebrahimi and Kleine [59] and Lenze and Günther [62]) has developed an analysis procedure similar to that described here to predict the fall off of the centerline conserved scalar concentration. Ebrahimi and Kleine [59] have shown that this analysis gives accurate predictions of ζ along the jet centerline for $20 < z/r_o < 100$ when ρ_∞ was assumed to be that for heated combustion gases ($T_f = 1600$ K, $\rho_f/\rho_\infty = 4.9$).

For larger downstream distances ζ was found to fall off more quickly than predicted. The authors attributed this to a buoyancy effect (i.e., an increase in jet momentum). However, it is possible that the analysis fails due to changes in the radial density profiles which invalidate the conditions for which eq (2) was derived. As figure 22 shows, the radial density profiles for the hydrocarbon flame are greatly modified at large downstream distances (e.g., $z/r_o = 160$). Such radial profiles cannot be considered as that of either a heavy jet into light surroundings or for a constant density jet. In order to predict the centerline behavior of ζ in this flow region it may be necessary to have a better understanding of the effects of local density

variations on turbulent mixing. Further experimentation is required to clarify the roles buoyancy-induced momentum and radial density profiles on turbulent mixing.

For regions of turbulent jet flames where direct comparisons of isothermal mixing results are valid, it should also be possible to predict centerline values of unmixedness. Measurements of unmixedness in several different jet flames are available [59-61,63]. These suggest that unmixedness levels in turbulent jet diffusion flames are of the same order as measured in isothermal flows, but there are systematic variations in most of the measurements which make direct quantitative comparison impossible.

As the above discussion suggests, isothermal measurements in variable density flows can provide important insights into the mixing behaviors of turbulent jet diffusion flames. Further work is required to determine for which conditions direct comparisons are valid and when it will be necessary to allow for local radial density variations due to the heat release of combustion.

4.4 Reynolds Number Effects in Diffusion Flames

The investigation of Re effects on mixing in variable density flows has important implications for mixing in turbulent jet diffusion flames [54]. It is well known that local Reynolds numbers, Re_l, for turbulent flames are much lower than calculated based on the room temperature properties of the flow at the nozzle. This is due to the large increase in kinematic viscosity which occurs when gases are heated.

The isothermal studies [34] have shown that the centerline mixing behavior is independent of Re except for downstream shifts in virtual origins

31

and longer flow distances required to attain asymptotic values of unmixedness which are found with increasing Re. This suggests that the mixing behavior of these turbulent flow fields is determined by large scale structures and that as long as the local Reynolds number is high enough to insure the development of large scale vortices, mixing in combustion regions of the flow field will be independent of Re_l. This conclusion is supported by the observations of Becker and Yamazaki [64] who noted that flame lengths of turbulent jet diffusion flames were independent of Re_l even when the turbulent structure was "fairly primitive, having little more than an appropriate large-eddy structure".

For isothermal flows it has been shown that centerline unmixedness attains asymptotic behavior over shorter flow distances at lower Re. This suggests that for the lower Re characteristic of combusting flows, the flow field should be able to respond to density fluctuations resulting from heat release over relatively short flow distances. This conclusion may be very helpful in understanding and predicting the effects of local density variations on mixing in complex chemically reacting flows.

5. SUMMARY

During the four years of this joint AFOSR/NBS research program significant progress has been made toward the goal of improving the understanding of chemically reacting turbulent flow. The results of experiments in this laboratory as well as measurements elsewhere on turbulent jet diffusion flames have justified the original choice to investigate flows having global density differences. It is anticipated that the experimental findings and the data base which were generated will be utilized by

32

researchers who are attempting to develop calculational procedures for describing chemically reacting flows. The real-time nature of the studies and the conclusion that vortical structures are modified by global density differences will be of particular interest for workers who are attempting to develop sophisticated calculational procedures to describe the time behavior of turbulent flows (e.g., see [65] and [66]).

During the past four years the use of Rayleigh light scattering for characterizing turbulent mixing behavior in isothermal, variable temperature, and combusting flows has become more widespread and many laboratories are now utilizing the technique. It is gratifying that the original careful characterization of the technique in this laboratory has contributed to this growth. It is anticipated that the development of new diagnostics for simultaneous point measurement of concentration and velocity and for line measurements of concentration will lead to further utilization of this unique and powerful technique.

REFERENCES

[1] Graham, S.C.; Grant, A.J.; and Jones, J.M. AIAA J. 12(8): 1140-1142; 1974 August.

[2] Dyer, T.M. AIAA J. 17(8): 912-914; 1979 August.

[3] Pitts, William M.; Kashiwagi, Takashi. The application of laser-induced Rayleigh light scattering to the study of turbulent mixing, Nat. Bur. Stand. (U.S.) NBSIR 83-2641; 1983 January. 114 p.

[4] Pitts, William M.; Kashiwagi, Takashi. J. Fluid Mech. 141: 391-429; 1984 April.

[5] Hinze, J.O. Turbulence. 2nd ed. New York: McGraw-Hill; 1975. 800 p.

[6] Schefer, R.W.; Dibble, R.W. AIAA J. 23(7): 1070-1078; 1985 July.

[7] Brown, G.L.; Rebollo, M.R. AIAA J. 10(5): 649-652; 1972 May.

[8] Way, J.; Libby, P.A. AIAA J. 34(8): 1567-1573; 1971 August.

[9] McQuaid, J.; Wright, W. Intl. J. Heat Mass Transfer. 17(2): 341-349; 1974 February.

[10] Pitts, William M.; McCaffrey, Bernard J.; Kashiwagi, Takashi. "A New Diagnostic for Simultaneous, Time-Resolved Measurements of Concentration and Velocity in Simple Turbulent Flow Systems," Presented at the Fourth Symposium on Turbulent Shear Flows, Karlsruhe, W. Germany; 1983 September 12-14.

[11] Pitts, William M.; McCaffrey, Bernard J. Response behavior of hot-wires and films to flows of different gases. Nat. Bur. Stand. (U.S.) NBSIR 85-3203; 1985 July. 123 p.

[12] Pitts, William M.; McCaffrey, Bernard J. J. Fluid Mech. 169: 465-512; 1986 August.

[13] Wu, P.; Libby, P.A. Intl. J. Heat Mass Transfer. 14(8): 1071-1077; 1971 August.

[14] McQuaid, J.; Wright, W. Intl. J. Heat Mass Transfer. 16(4): 819-828; 1973 April.

[15] Simpson, R.L.; Wyatt, W.G.; J. Phys. E: Sci. Instrum. 6(10): 981-987; 1973 October.

[16] Andrews, G.E.; Bradley, D.; Hundy, G.F. Intl. J. Heat Mass Transfer. 15(10): 1765-1786; 1972 October.

[17] Baum, Howard R.; McCaffrey, Bernard J.; Pitts, William M. unpublished work.

[18] Aldén, M.; Edner, H.; Holmstedt, G.; Svanberg, S.; Högberg, T. Appl. Optics. 21(7): 1236-1240; 1982 April 1.

[19] Escoda, M.C.; Long, M.B. AIAA J. 21(1): 81-84; 1983 January.

[20] Long, M.B.; Fourguette, D.C.; Escoda, M.C.; Layne, C.B. Optics Lett. 8(5): 244-246; 1983 May.

[21] Kychakoff, G.; Howe, R.D.; Hanson, R.K.; Drake, M.C.; Pitz, R.W.; Lapp, M.; Penney, C.M. Science. 224(4647): 382-384; 1984 April 27.

[22] Koochesfahani, M.M; Dimotakis, P.E. AIAA J. 23(11): 1700-1707; 1985 November.

[23] Yip, B.; Long, M.B. Optics Lett. 11(2): 64-65; 1986 February.

[24] Pitts, William M. Development of a line camera for real-time measurements of concentration in turbulent flow fields. Proceedings of the International Congress on Applications of Lasers and Electro-Optics: Flow and Particle Diagnostics; Vol. 58; The Laser Institute of America; 1986 November 10-13. 7-15.

[25] Gibson, C.H.; Friehe, C.A.; McConnell, S.O. Phys. Fluids. 20(10, pt. 2): S156-S167; 1977 October.

[26] Chevray, R. Prog. Energy Combust. Sci. 8(4): 303-315; 1982.

[27] Drake, M.C.; Shyy, W.; Pitz, R.W. Superlayer contribution to conserved scalar PDFS in a H_2 turbulent jet diffusion flame. Presented at the Fifth Symposium on Turbulent Shear Flows; Ithaca, New York; 1985 August 7-9.

[28] Drake, M.C.; Pitz, R.W.; Shyy, W. J. Fluid Mech. 171: 27-51; 1986 October.

[29] List, E.J. Mechanics of turbulent buoyant jets and plumes. Turbulent Jets and Plumes, W. Rodi, ed. New York: Pergamon Press; 1982. 1-68.

[30] Chen, C.J.; Rodi, W . Vertical turbulent buoyant jets--a review of experimental data. New York: Pergamon Press; 1980. 88 p.

[31] Antonia, R.A.; Prabhu, A.; Stephenson, S.E. J. Fluid Mech. 72(3): 455-480; 1975 December 9.

[32] Chevray, R.; Tutu, N.K. J. Fluid Mech. 88(1): 133-160; 1978 Septemer 13.

[33] Catalano, G.D.; Morton, J.B.; Humphris, R.R. AIAA J. 14(9): 1157-1158; 1976 September.

[34] Pitts, William M. Effects of global density and Reynolds number variations on mixing in turbulent, axisymmetric jets. Nat. Bur. Stand. (U.S.) NBSIR 86-3340; 1986. 172 p.

[35] Thring, M.W.; Newby, M.P. Combustion length of enclosed turbulent jet flames. Fourth symposium (intl) on combustion. Pittsburgh, PA: The Standing Committee on Combustion; 1953. 789-796.

[36] Sunavala, P.D.; Hulse, C.; Thring, M.W. Com. Flame. 1(2): 179-193; 1972 June.

[37] Wilson, R.A.M.; Danckwerts, P.V. Chem. Eng. Science. 19: 885-895; 1964.

[38] Bilger, R.W. Prog. Energy Com. Science. 1(2/3): 87-109; 1976.

[39] Williams, F.A. Combustion Theory, 2nd ed. Reading, MA: Benjamin/Cummings; 1985. 680 p.

[40] Effelsberg, E.; Peters, N. Com. Flame. 50(3): 351-360: 1983 April.

[41] Gibson, C.H.; Chen, C.C.; Lin, S.C. AIAA J. 6(4): 642-649; 1968 April.

[42] Screenivasan, K. R.; Tavoularis, S. J. Fluid Mech. 101(4): 783-795; 1980 December 29.

[43] Vanquickenborne, L.; van Tiggelen, A. Com. Flame. 10(1): 59-69; 1966 March.

[44] Hall, L.; Horch, K.; Günther, R. Brennstoff-Wärme-Kraft. 32(1): 26-31; 1980 January.

[45] Günther, R.; Horch, K.; Lenze, B. The stabilization mechanism of free jet diffusion flames. First specialist meeting (intl) of the combustion institute. Pittsburgh, PA: The Combustion Institute; 1981. 117-122.

[46] Eickoff, H.; Lenze, B.;, and Leuckel, W. Experimental investigation on the stabilization of jet diffusion flames. Twentieth symposium (intl) on combustion. Pittsburg, PA: The Combustion Institute; 1984. 311-318.

[47] Kalghatgi, G.T. Com. Science. Tech. 41(1+2): 17-29; 1984.

[48] Byggstøyl, S.; Magnussen, B.F. A model for flame extinction in turbulent flow. Turbulent Shear Flows 4, eds. Bradbury, L.J.S. et al., Springer-Verlag, Berlin; 1985. 381-395.

[49] Janicka, J.; Peters, N. Prediction of turbulent jet diffusion flame lift-off using a PDF transport equation. Nineteenth symposium (intl) on combustion. Pittsburg, PA: The Combustion Institute; 1982. 367-374.

[50] Peters, N.; Williams, F.A. AIAA J. 21(3): 423-429; 1983 March.

[51] Peters, N. Partially premixed diffusion flamelets in non-premixed turbulent combustion. Twentieth symposium (intl) on combustion. Pittsburgh, PA: The Combustion Institute; 1984. 353-360.

[52] Broadwell, J.E.; Dahm, W.J.A.; Mungal, M.G. Blowout of turbulent diffusion flames. Twentieth symposium (intl) on combustion. Pittsburgh, PA: The Combustion Institute; 1984. 303-310.

[53] Kalghatgi, G.T. Com. Science Tech. 26(5 and 6): 233-239; 1981.

[54] Pitts, William M. The effects of global density and Reynolds number variations on mixing in turbulent, axisymmetric jets--implications for turbulent jet diffusion flames. Proceedings of the 2nd ASME/JSME Joint Thermal Engineering Conference, Book #10219S, Volume 1; Honolulu, HI 1987 March 23-27.

[55] Sobiesiak, A.; Brzustowski, T.A., On the structure of the stabilization region of lifted turbulent diffusion flames. Presented at the 1986 Spring Meeting of the Western States Section of the Combustion Institute, Banff, Canada; 1986 April 27-30.

[56] Wohl, K.; Gazley, C.; Kapp, N. Diffusion Flames. Third symposium on combustion, flame, and explosion phenomena. Baltimore, MD: Williams and Wilkins; 1949. 288-300.

[57] Savas, Ö.; Gollahalli, S.R. AIAA J. 24(7): 1137-1140; 1986 July.

[58] Chigier, N.A.; Strokin, V. Com. Science Tech. 9(3 and 4): 111-118; 1974.

[59] Ebrahimi, I.; Kleine, R. The nozzle fluid concentration fluctuation field in round turbulent free jets and jet diffusion flames. Sixteenth symposium (intl) on combustion. Pittsburgh, PA: The Combustion Institute; 1977. 1711-1723.

[60] Kennedy, I.M.; Kent, J.H. Measurements of a conserved scalar in turbulent jet diffusion flames. Seventeenth symposium (intl) on combustion. Pittsburgh, PA: The Combustion Institute; 1979. 279-287.

[61] Drake, M.C.; Bilger, R.W.; and Stårner, S.H. Raman measurements and conserved scalar modeling in turbulent diffusion flames. Nineteenth symposium (intl) on combustion. Pittsburgh, PA: The Combustion Institute; 1982. 459-467.

[62] Lenze, B. and Günther, R. Brennstoff-Wärme-Kraft. 27(10): 387-394; 1975 October.

[63] Günther, R. Prog. Energy Com. Science. 9(1/2): 105-154; 1983.

[64] Becker, H.A. and Yamazaki, S. Com. Flame. 33(2): 123-149; 1978.

[65] Grinstein, F.F.; Oran, E.S.; Boris, J.P. AIAA J. 25(1): 92-98; 1987 January.

[66] Ghoniem, A.F. and Sethian, J.A. AIAA J. 25(1): 168-171: 1987 January.

[67] Lockwood, F.C. and Moneib, H.A. Com. Flame. 47(3): 291-314; 1982 September.

TABLE 1

Experimental Parameters

Jet/Coflow	ρ_o/ρ_∞	Re	Experiments (R = Rayleigh, S = Shadowgraph)
He/air	0.14	3950	R,S
CH_4/air	0.55	3950	R,S
C_3H_8/CO_2	1.02	3960	R,S
C_3H_8/air	1.55	3960	R,S
C_3H_8/air	1.55	7890	R,S
C_3H_8/air	1.55	11860	R,S
CF_4/air	3.01	3960	R
CF_4/air	3.01	7920	R
SF_6/air	5.11	3950	R,S
SF_6/air	5.11	7890	R,S
SF_6/air	5.11	11860	R,S
SF_6/He	37.0	3960	R,S

FIGURE CAPTIONS

Figure 1. The experimental configuration for real-time Rayleigh light scattering "point" measurements of concentration in binary gas mixtures is shown schematically. The flow system consists of a 6.35 mm diameter pipe with a sharpened edge enclosed within a 100 X 100 cm^2 square cylinder.

Figure 2. The quality of the data which can be acquired utilizing the Rayleigh light scattering technique for concentration is demonstrated. Radial profiles of concentration (in both mole and mass fraction terms) are plotted for a turbulent CH_4 jet flowing into a slow coflow of air. The downstream distance is $z/r_o = 35$ and the Reynolds number is 3950.

Figure 3. Partial time-resolved data records recorded during a simultaneous Rayleigh light scattering and hot-film anemometry experiment are reproduced for a propane jet (Re = 3960) flowing into a slow coflow of air. The observation volume is located on the jet centerline at $z/r_o = 31.5$. The light scattering signals have been calibrated and are plotted in terms of mole fraction of propane. The raw data for the anemometer output is plotted along with the velocity calculated utilizing the calibrations of film response to changes in velocity and gas composition.

Figure 4. The correlation is shown for the heat transfer from a hot-wire as a function of flow velocity for nine different gases. Experimental measurements are nondimensionalized by the use of the Nusselt number and Reynolds number. Corrections have been included for heat losses to the prongs of the hot-wire and thermal slip and accommodation effects at the surface of the probe. $(K_B)_x$ and $(K_A)_x$ are coefficients which are necessary to compensate for variations in molecular properties from gas to gas.

Figure 5. The camera which has been developed for recording real-time Rayleigh light scattering intensity along a line is shown. The top portion indicates the major components and their configuration. The actual appearance of the camera is shown below.

Figure 6. The overall experimental configuration for real-time measurements of concentration along a line in turbulent flows is represented. Rayleigh light scattering is induced along a line in the flow field by the Ar^+ ion laser. Light scattering at 90° is recorded by the digital line camera system consisting of the line camera shown in figure 5, suitable interfaces, and a data acquisition minicomputer.

Figure 7. An example of time-resolved line measurements of propane mole fraction across a turbulent jet of propane (Re = 3960) flowing into a coflow of air is reproduced. Propane mole fraction is represented by a seven level gray scale. The downstream position is 5 diameters and the line read out rate is 830 Hz.

Figure 8.   Time-averaged radial profiles of propane mole fraction are shown
            for five downstream positions in the development region of a
            propane (Re = 3960) jet flowing into a slow coflow of air. The
            growth of the boundary layers on either side of the potential core
            with increasing z and decrease of centerline concentration at the
            end of the potential core can be clearly observed. It is
            interesting to note that the data displayed represents 164,000
            individual concentration measurements which were recorded during
            1.54 s of actual acquisition time.

Figure 9.   The apparatus for recording time-resolved shadowgraphs is
            represented schematically. The light pulse generated by the
            chopper has a temporal profile which is triangular in shape and has
            a total duration of 310 μs.

Figure 10. Three time-resolved shadowgraphs are shown for a SF_6 jet (Re =
            3950) flowing into a slow coflow of air. Three different
            downstream positions recorded at different times are represented.
            Note particularly the formation of a fountain by the SF_6 at a
            downstream position of $\approx$ 37.5 r_o.

Figure 11. Shadowgraphs are reproduced for jets of SF_6 (Re = 7890 and 11,860)
            entering slow coflows of air. For each jet four views of the flow
            recorded at different times and positions in the jet are
            superimposed. Note that the fine scale turbulence becomes more
            pronounced with increasing Re, but that the overall spreading rate
            of the jet does not appear to be affected.

Figure 12. Five sets of superimposed shadowgraphs are shown for jets of one
            gas flowing into a second gas. With the exception of the SF_6
            flow, the Reynolds numbers are roughly the same. The effects of
            variations in the global density ratio appear as changes in the
            development region of the flow and modifications in the eddy
            structure at downstream positions where the flows are close to
            fully-developed.

Figure 13. Superimposed shadowgraphs are reproduced for propane jets at three
            Re entering into slow coflows of air. The development of finer
            turbulent scales with increasing Re can be clearly seen. It is
            also evident that increasing the Re results in a shortening of the
            distance required for the development of vortical structures near
            the nozzle. The overall spreading behavior of the jets is
            independent of Re supporting the supposition that entrainment is
            determined by large scale turbulent structures.

Figure 14. Values of $Y_o/\overline{Y}_m$ ($\overline{Y}_c = \overline{Y}_m$ is the centerline concentration at z/r_o
            and Y_o is the mass fraction of jet fluid at the jet exit) are
            plotted as a function of z/r_o for six different jet/coflow gas
            combinations. The solid lines are linear least squares fits of
            the results. Note the decreasing slopes and upstream movement of

            the virtual origins (z where $Y_o/\overline{Y}_c \rightarrow 0$) which occur as the
            jet/coflow density ratio is increased.

Figure 15.   Predicted values of inverse centerline mass fraction (denoted as $1/C_m$) based on the analysis of Thring and Newby [35] are plotted as functions of z/r_o for the six jet/coflow gas pairs which have been experimentally investigated. Comparison of figures 14 and 15 shows that there is good agreement between prediction and experiment.

Figure 16.   Values of centerline unmixedness are plotted as a function of z/r_o for the six jet/coflow gas pairs listed. Values of $Y_m'/\bar{Y}_m$ for each jet approach a common asymptote of ≈ 0.23, but the flow distance required increases dramatically as the jet/coflow density ratio increases.

Figure 17.   The centerline unmixedness values shown in figure 16 are replotted as a function of z/r_ϵ. The collapse of the data onto a single curve suggests that r_ϵ is the proper scaling parameter for correlating the growth of unmixedness in these variable density flows.

Figure 18.   Centerline unmixedness values for three different Re jets of propane entering slow coflows of air are plotted as functions of z/r_o. Flows at higher Re require longer flow distances in order to achieve the asymptotic value of unmixedness even though the value of the asymptote does not change.

Figure 19.   The concentration contour corresponding to that for which the laminar flame speed of an ethylene/air mixture is a maximum ($Y_1 = 0.073$) is plotted as functions of z/r_o and r/r_o. The virtual origin for the plot is assumed to be at $z = 0$. Two representations are shown. On the right the radial and axial axes have the same scaling, while on the left the radial scale is expanded by a factor of 5.

Figure 20.   Experimental values [47] of lift-off height (h) are plotted against jet exit velocity for turbulent jet flames of methane, ethylene, and propane. These measured values are compared with values (solid lines) predicted using eq. (5) and the known velocity and mixing behaviors of the jets. The agreement is excellent.

Figure 21.   Experimental [53] (symbols) and calculated values (lines) of blow out velocity are plotted as a function of jet radius for axisymmetric turbulent jet flames of five organic fuels. Calculated values are derived by using eqs. (6) and (7). The agreement of the predicted values with experiment is very good.

Figure 22.   Approximate radial density profiles for three nondimensional downstream distances are shown for turbulent jet diffusion flames of hydrogen and a typical organic fuel (methane). These curves are based on measurements reported by several different authors [63,67].
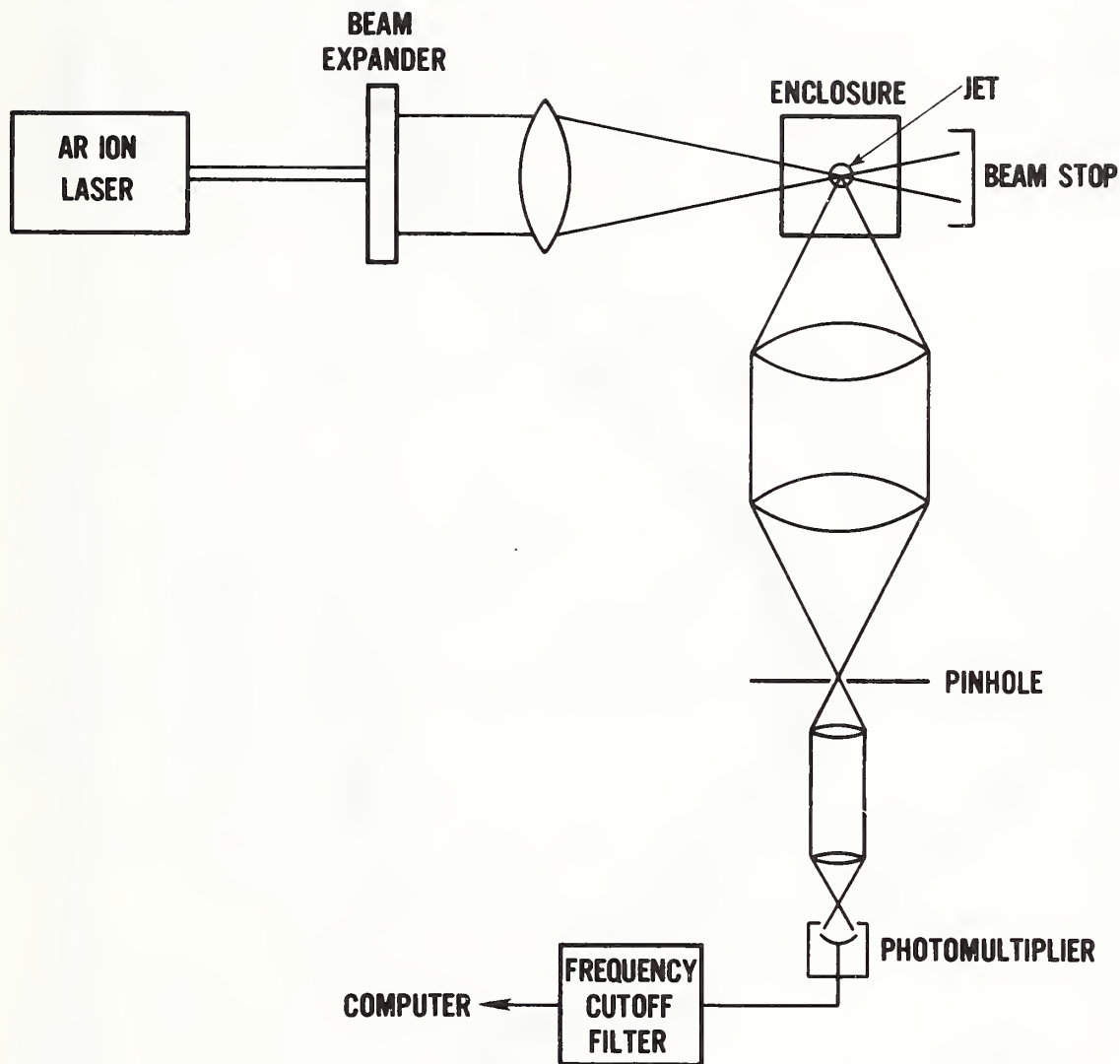
Figure 1. The experimental configuration for real-time Rayleigh light scattering measurements of concentration.
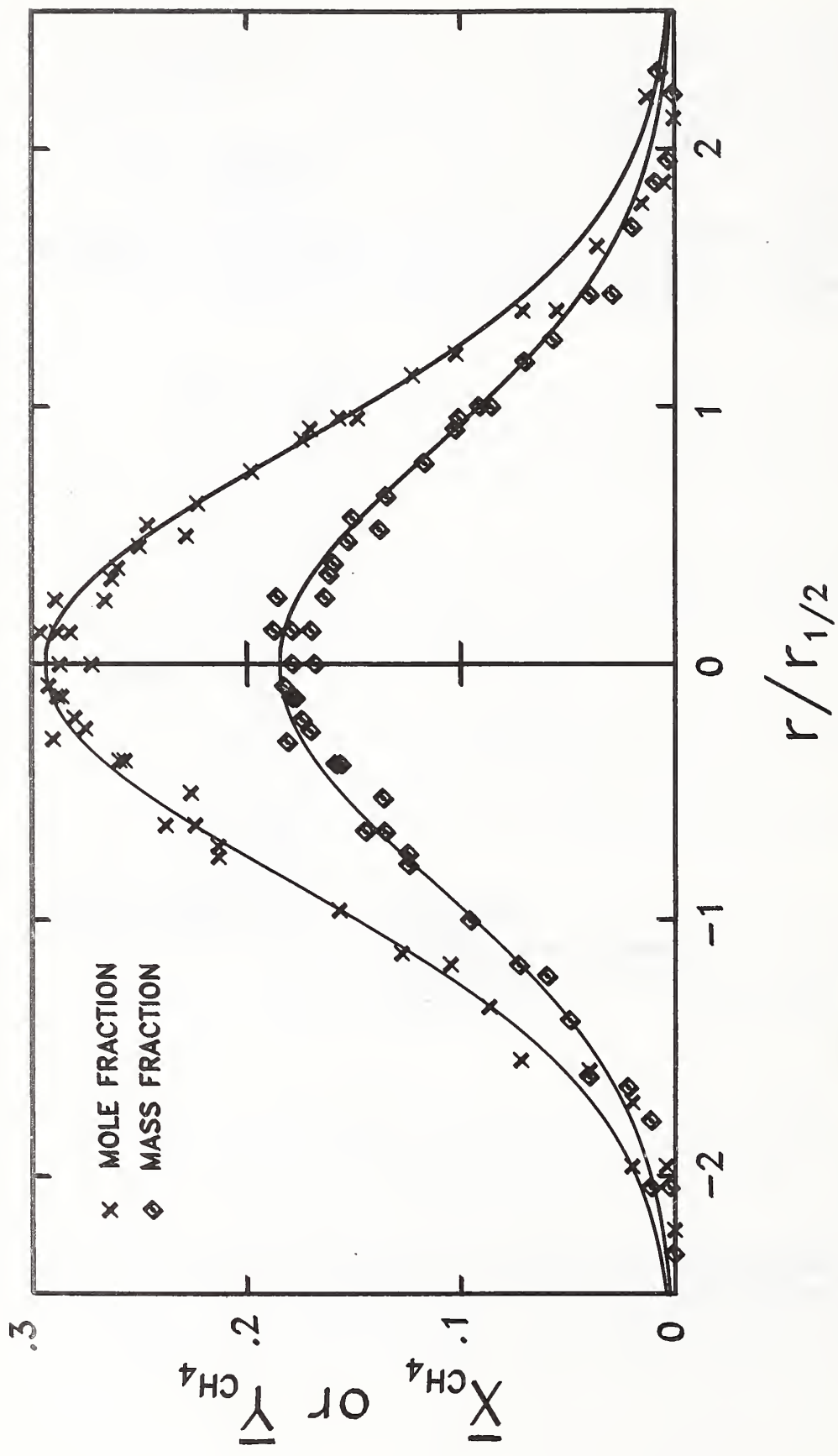
Figure 2. Radial profiles of concentration are plotted for a turbulent CH_4 jet flowing into a slow coflow of air.
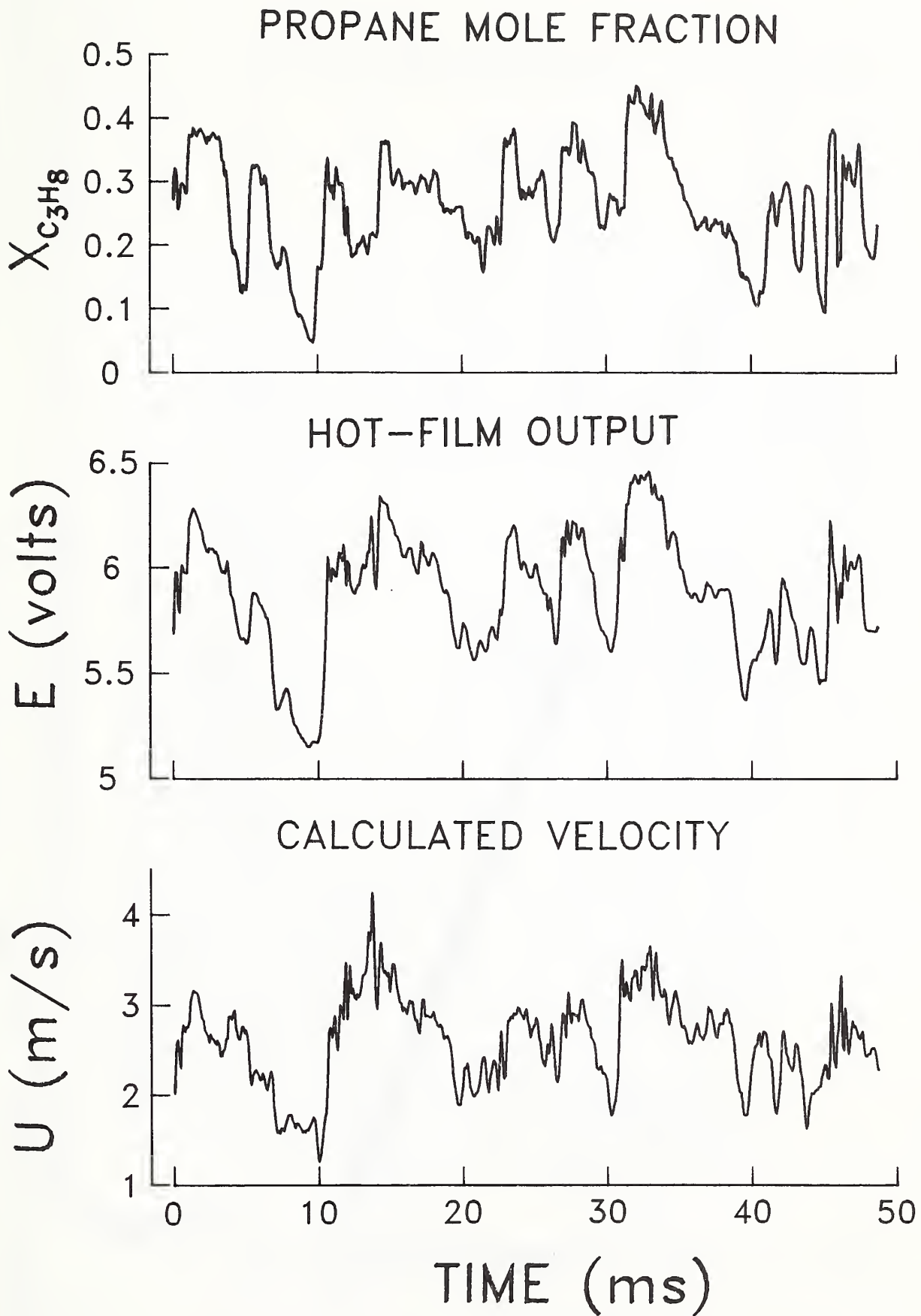
Figure 3. Partial time-resolved data records recorded during a simultaneous Rayleigh light scattering and hot-film anemometry experiment.
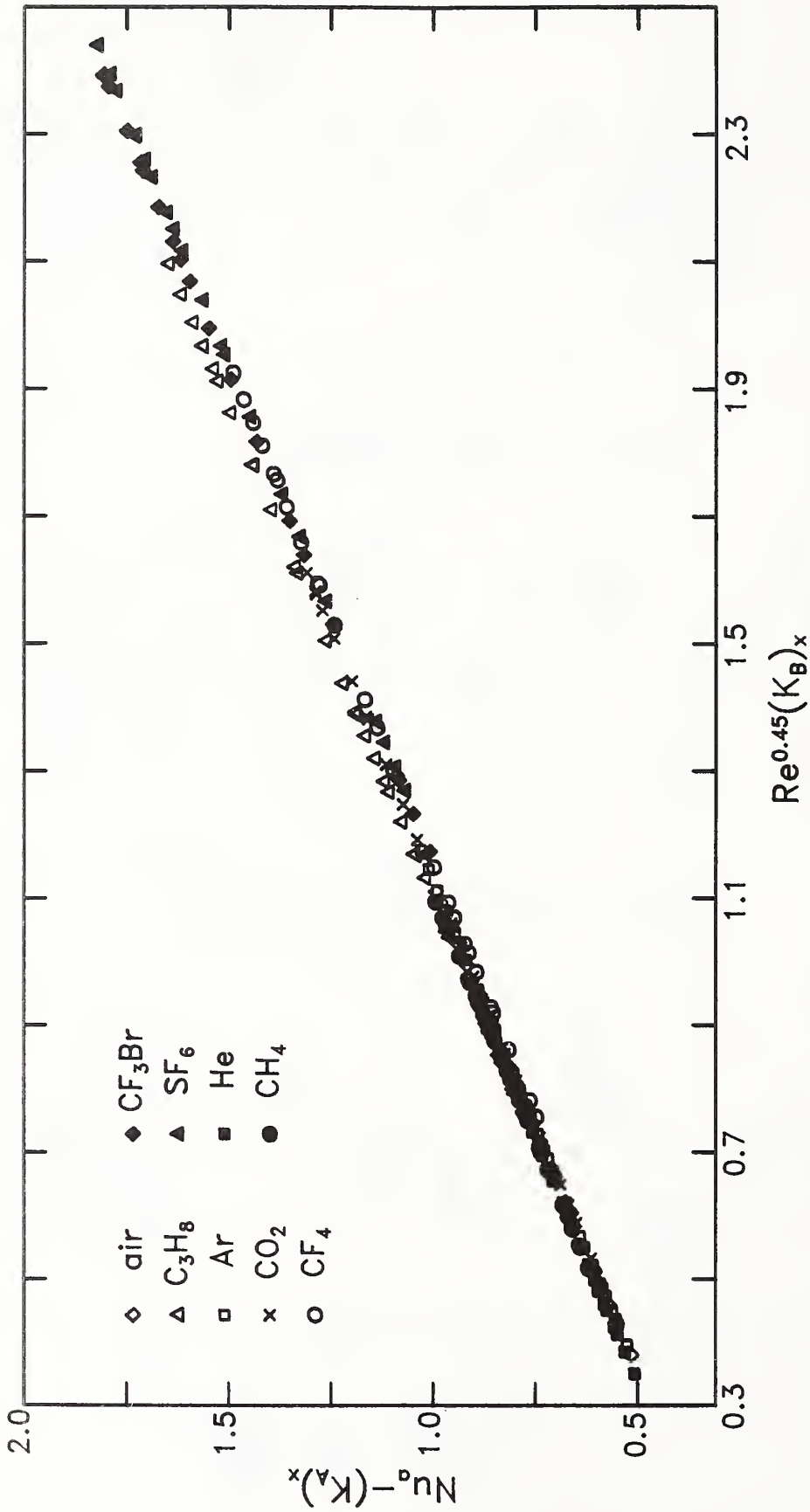
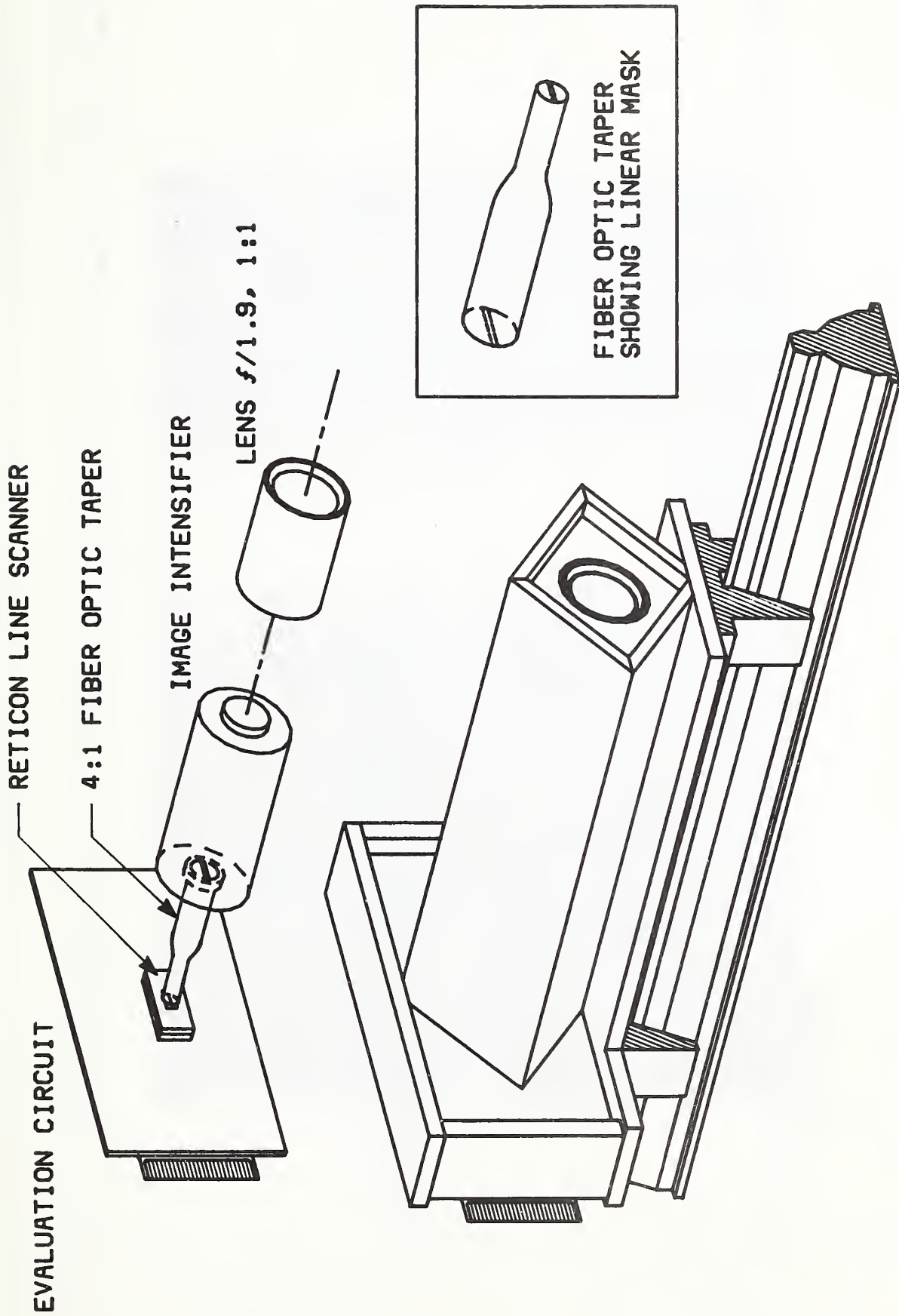Figure 4. The correlation is shown for the heat transfer from a hot-wire as a function of velocity for nine different gases.

EVALUATION CIRCUIT

RETICON LINE SCANNER

4:1 FIBER OPTIC TAPER

IMAGE INTENSIFIER

LENS ƒ/1.9, 1:1

FIBER OPTIC TAPER
SHOWING LINEAR MASK

Figure 5. The camera for recording real-time Rayleigh light scattering intensity along a line is shown.
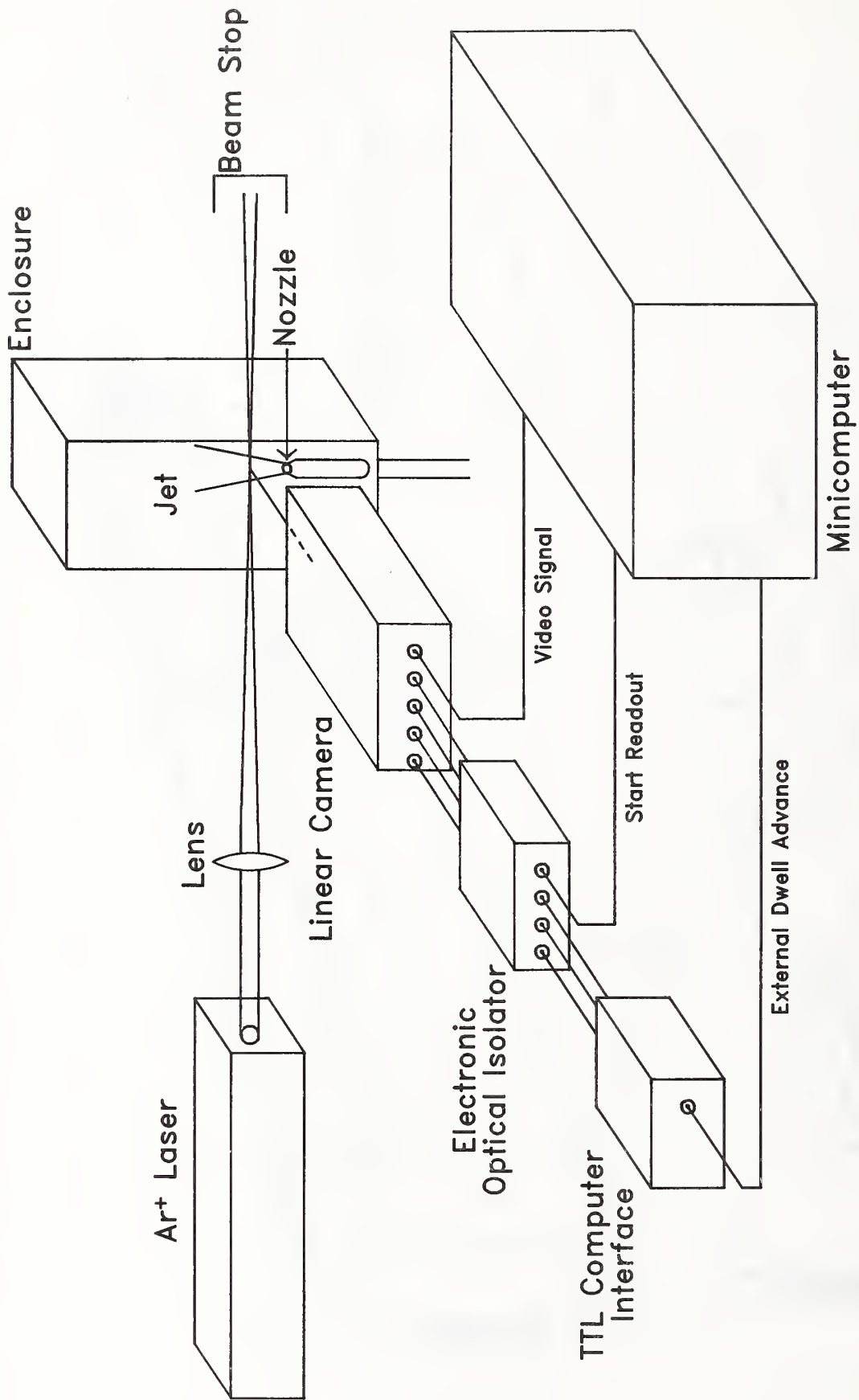
47

Figure 6. The overall experimental configuration for real-time measurements of concentration along a line in turbulent flows.
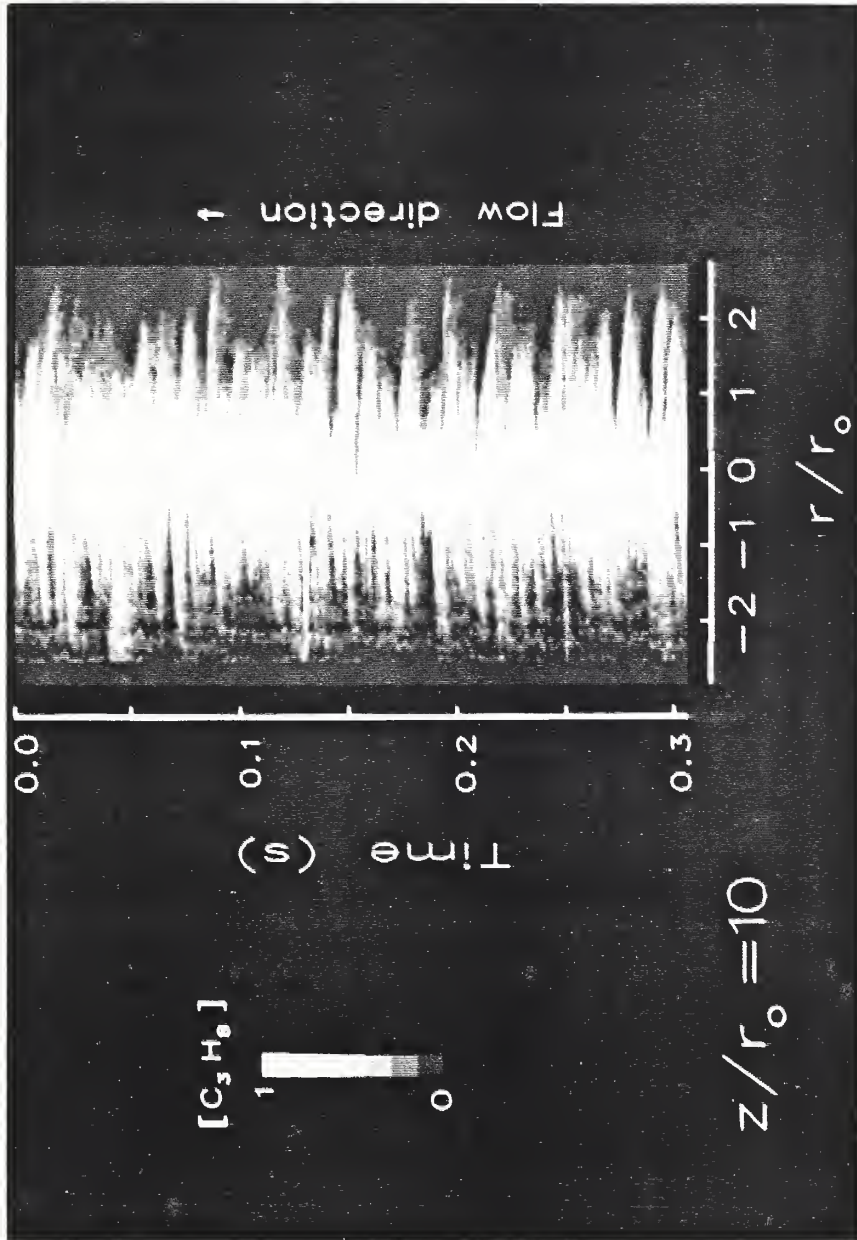
Figure 7. An example of time-resolved line measurements of mole fraction across a turbulent jet of C_3H_8.
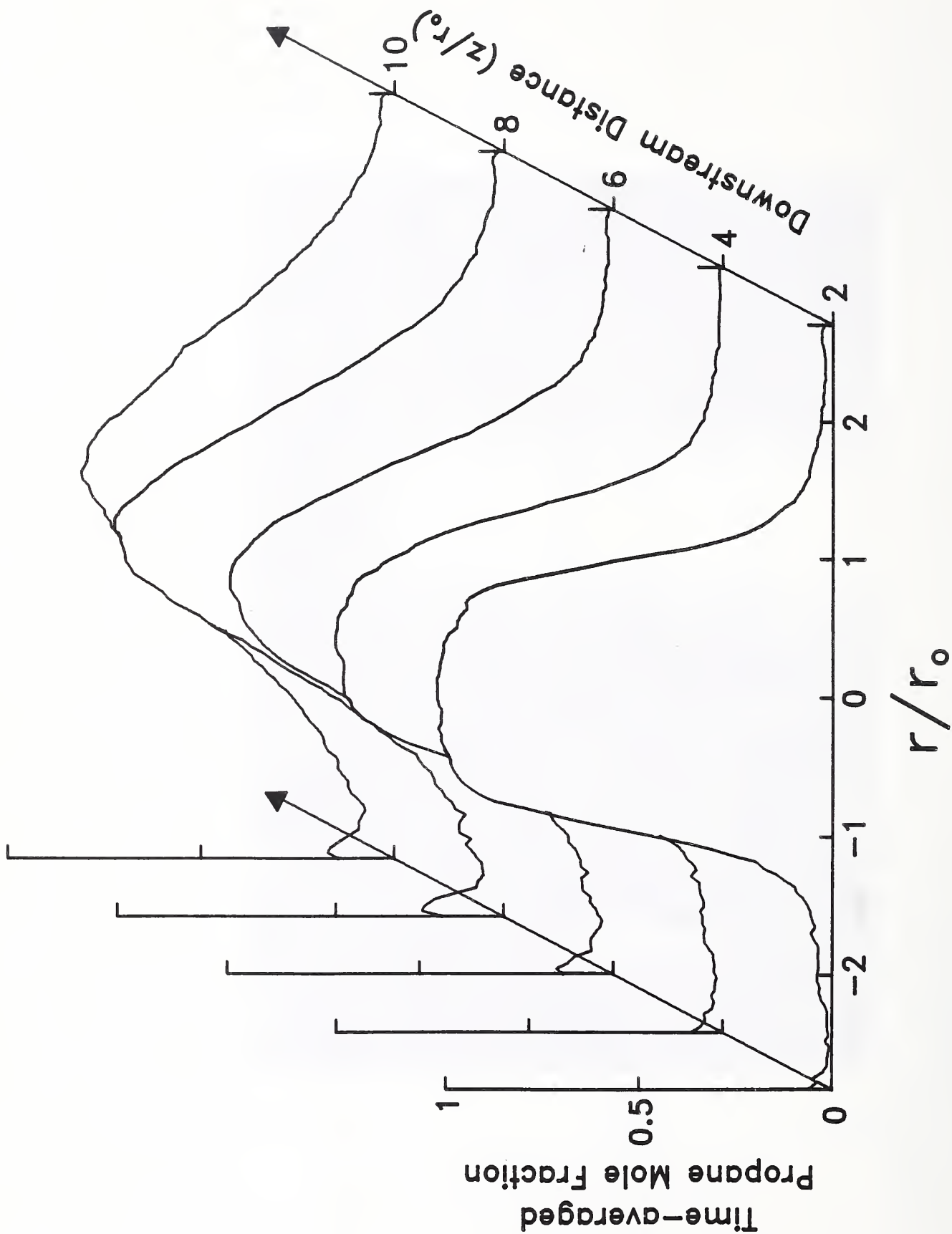
Figure 8.   Time-averaged radial profiles of mole fraction are shown for a propane jet flowing into air.
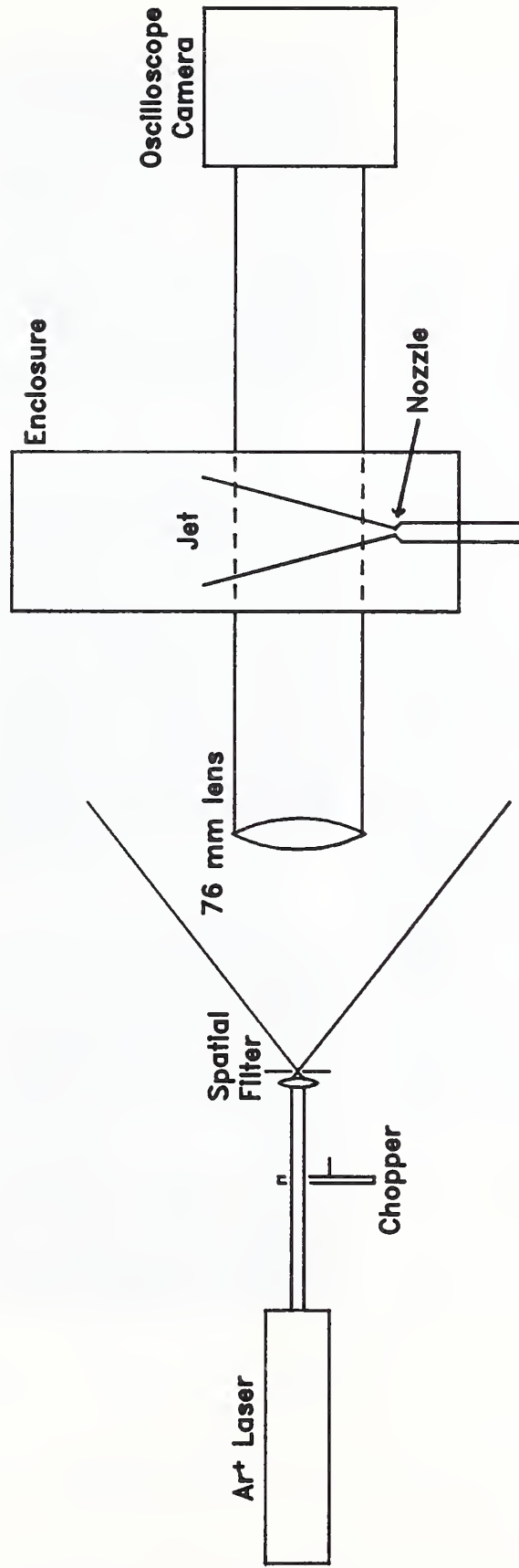
Figure 9. The apparatus for recording time-resolved shadowgraphs is represented schematically.
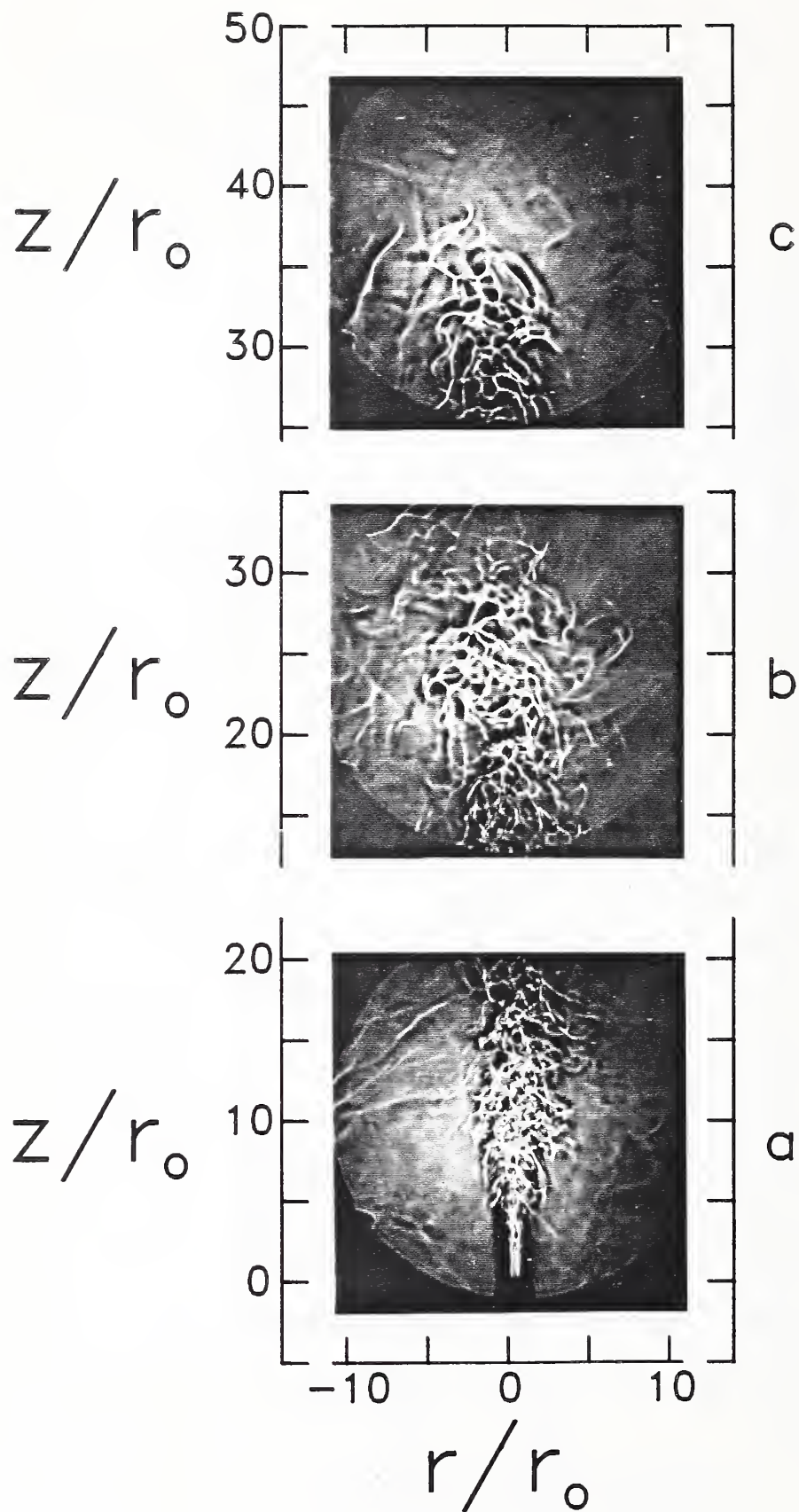
Figure 10.   Three time-resolved shadowgraphs are shown for a SF_6 jet (Re = 3950) flowing into a slow coflow of air.
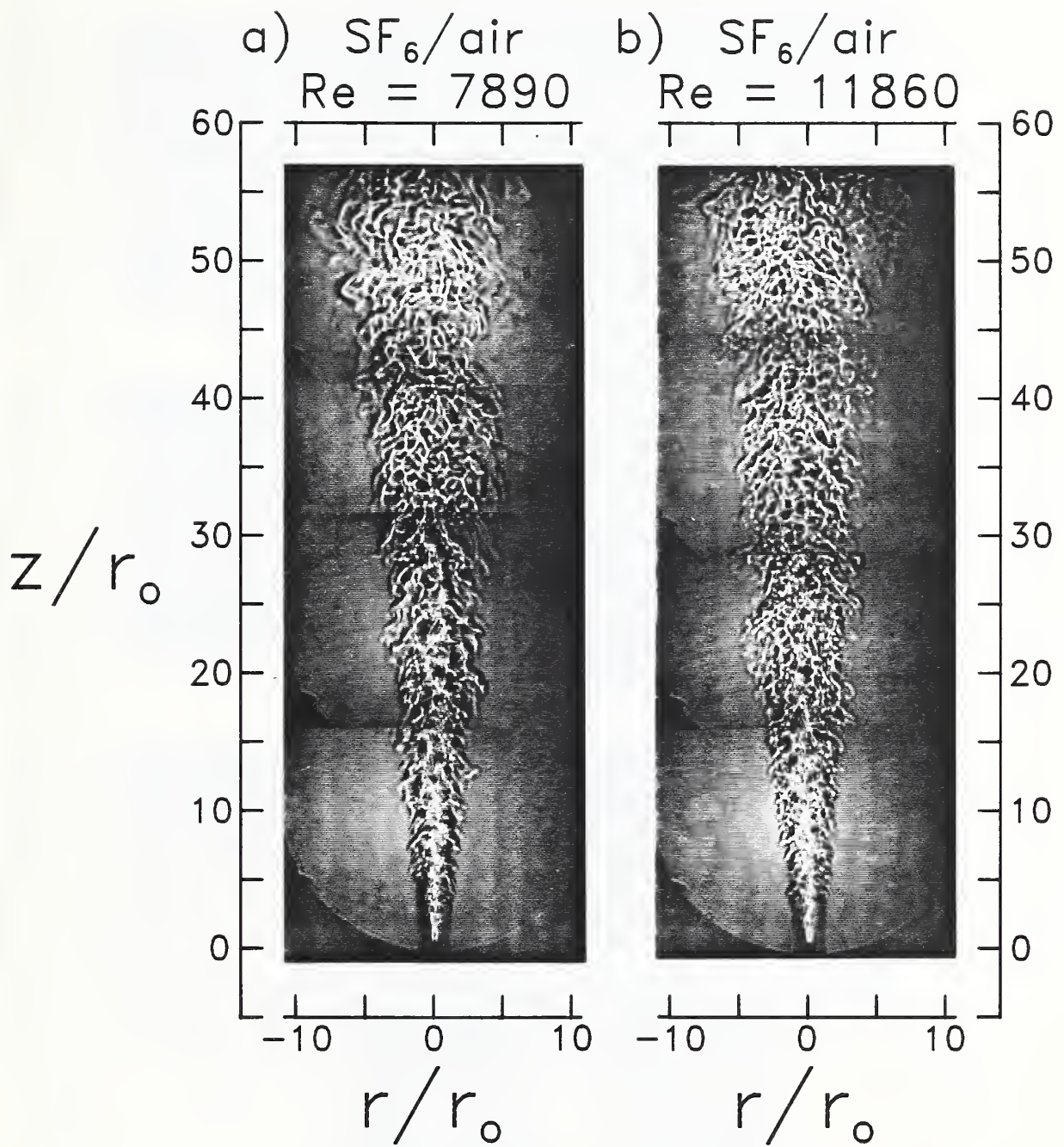
Figure 11. Shadowgraphs are reproduced for jets of SF_6 entering slow coflows of air.
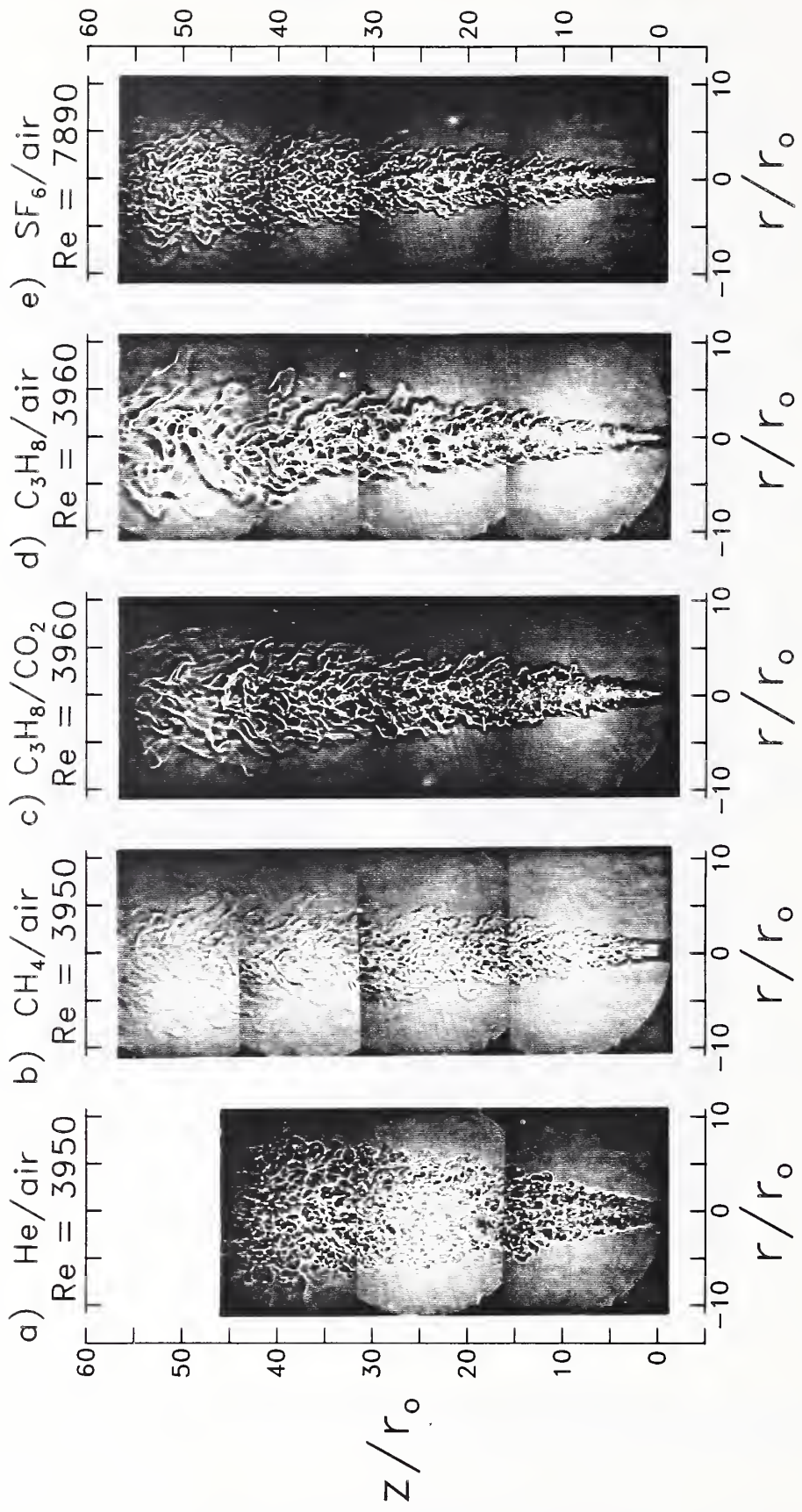
Figure 12. Superimposed shadowgraphs are shown for jets of one gas flowing into a second gas.
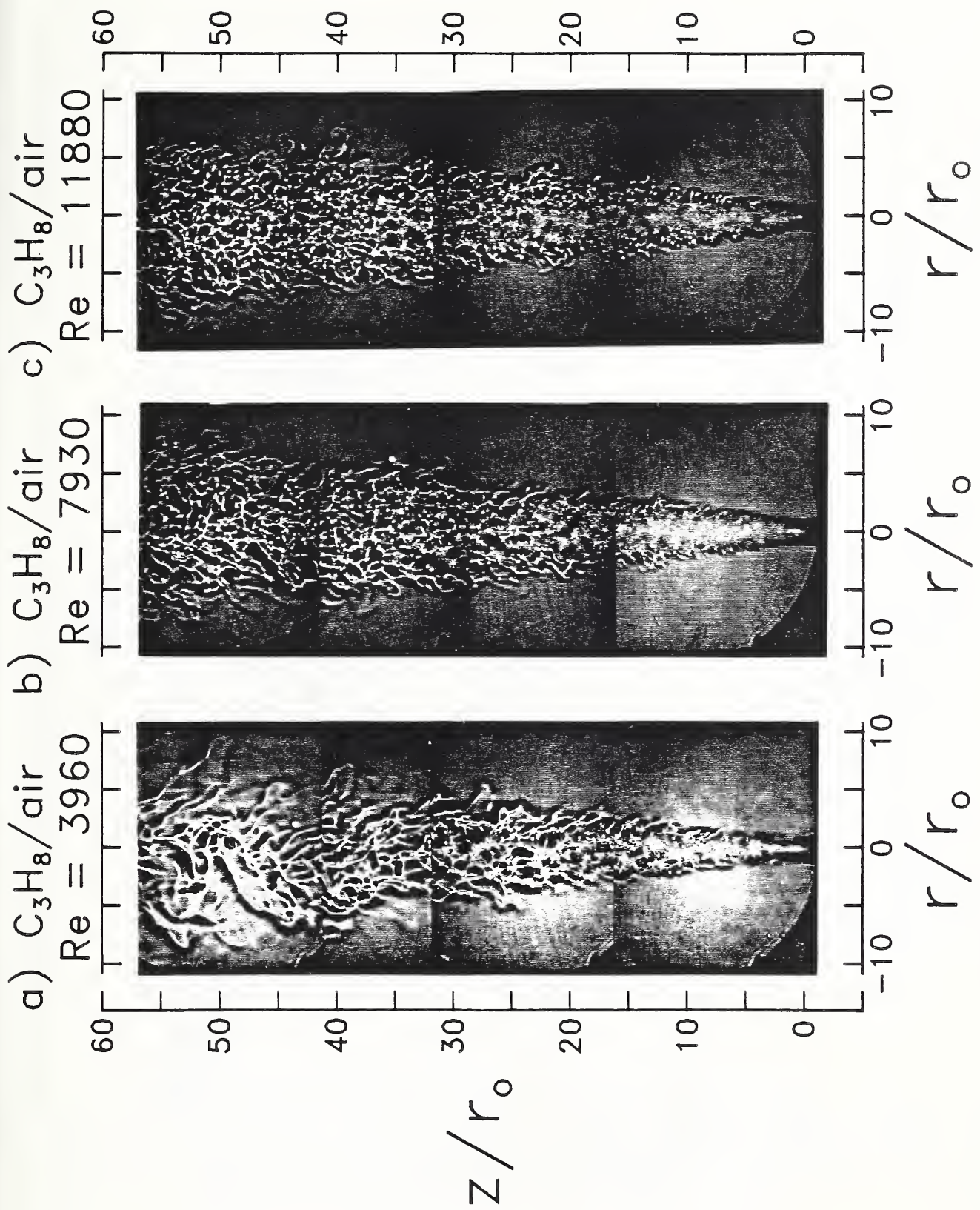
Figure 13. Superimposed shadowgraphs for propane jet at three Re entering slow coflows of air.
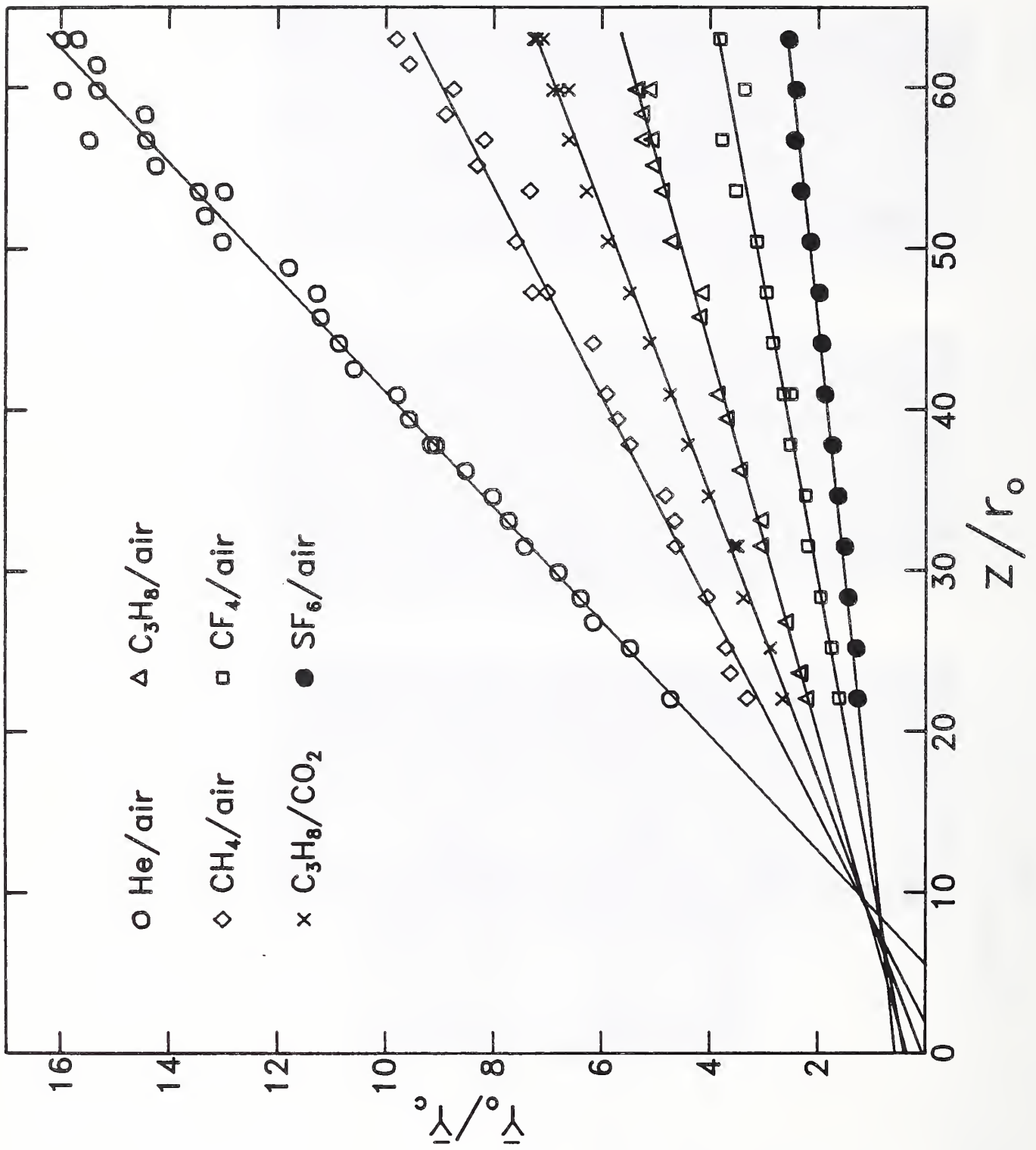
55

Figure 14. Values of $Y_o/\overline{Y}_m$ are plotted as a function of z/r_o for six different jet/coflow gas combinations.

Legend:
- ○ He/air
- △ C_3H_8/air
- ◇ CH_4/air
- □ CF_4/air
- × C_3H_8/CO_2
- ● SF_6/air
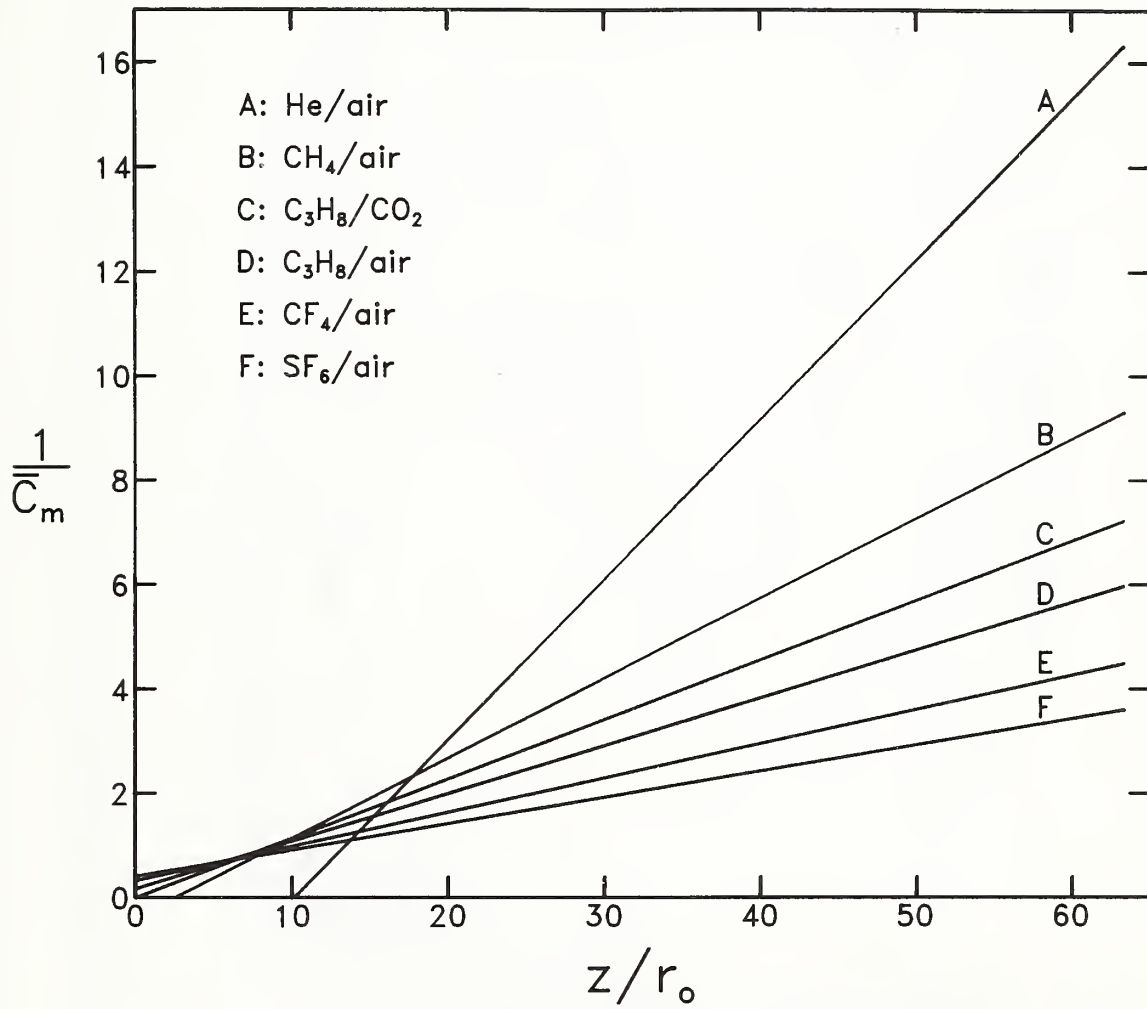
Figure 15. Predicted values of inverse centerline mass fraction based on the analysis of Thring and Newby.
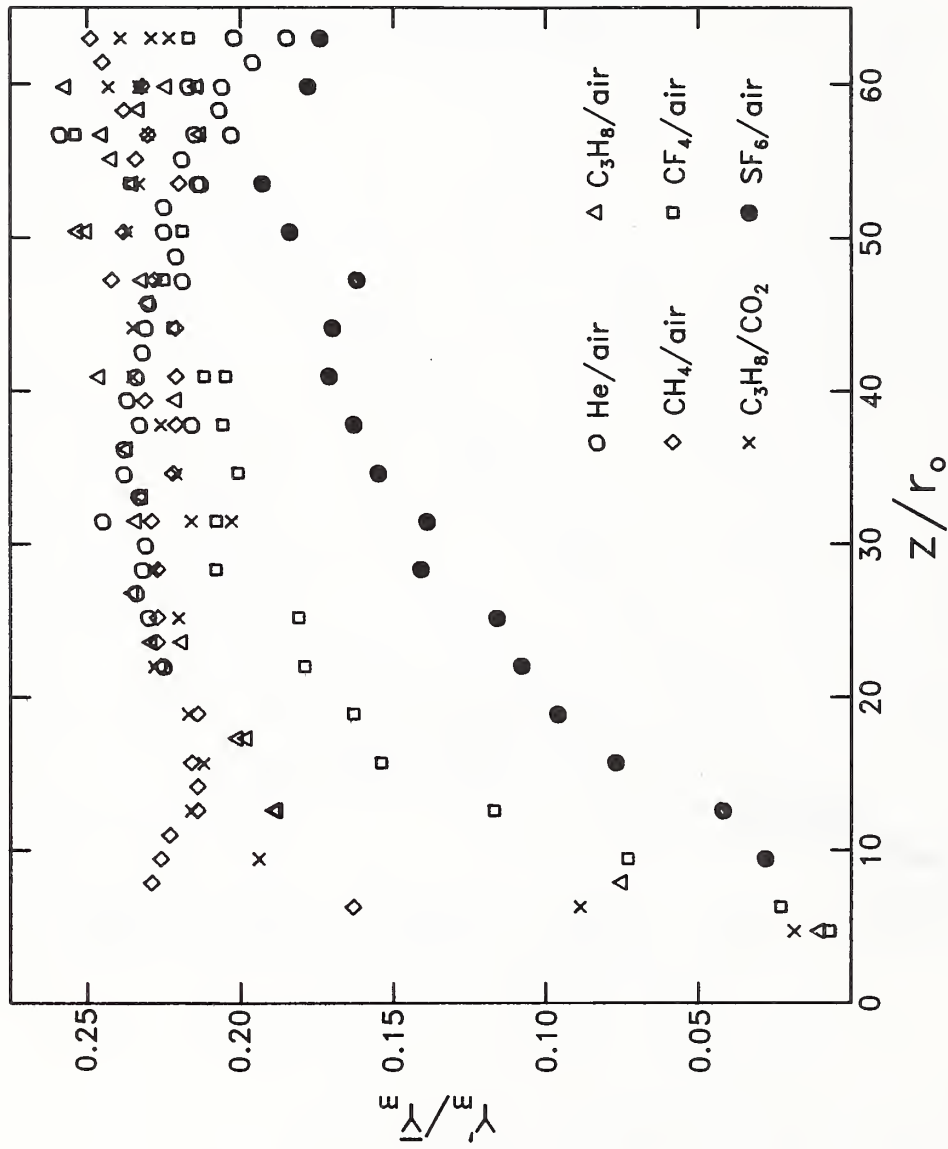
Figure 16. Values of centerline unmixedness are plotted as a function of z/r_o for the jet/coflow pairs listed.
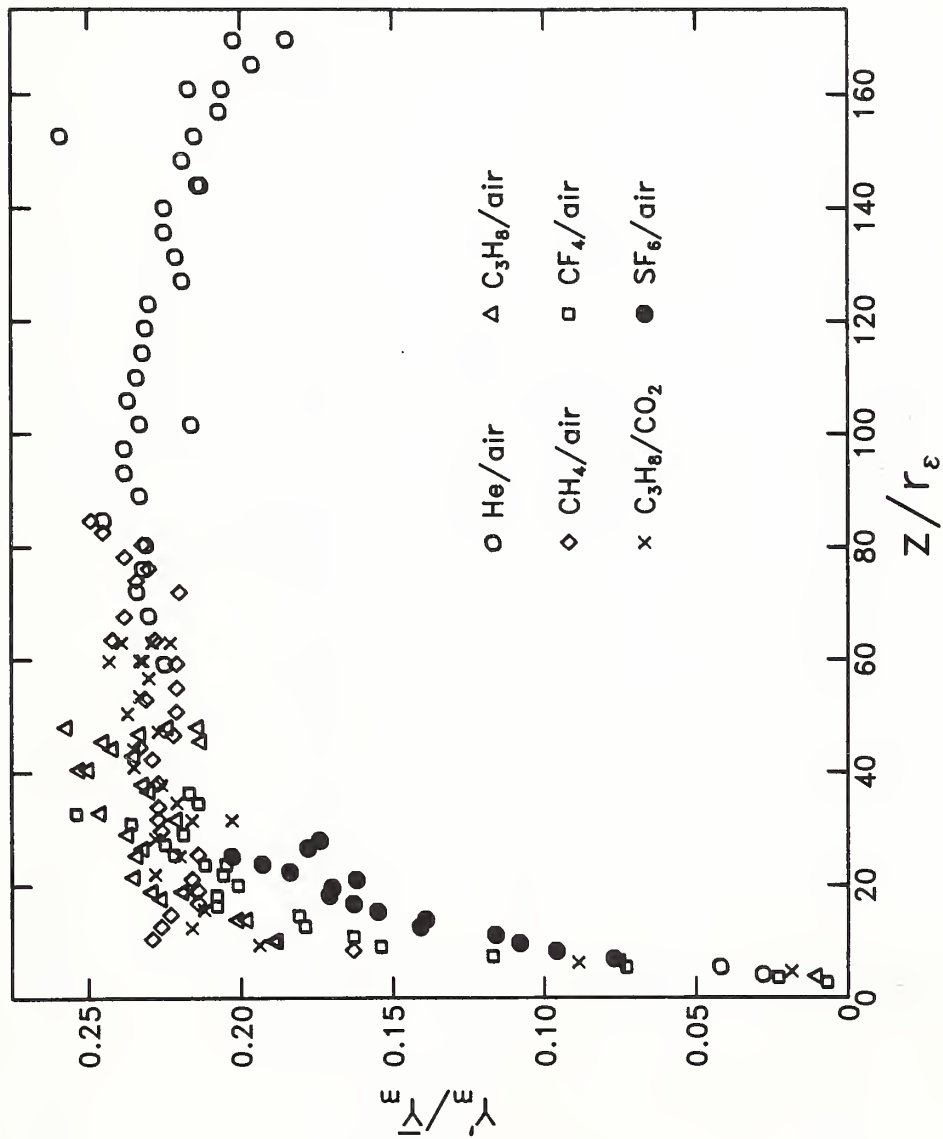
58

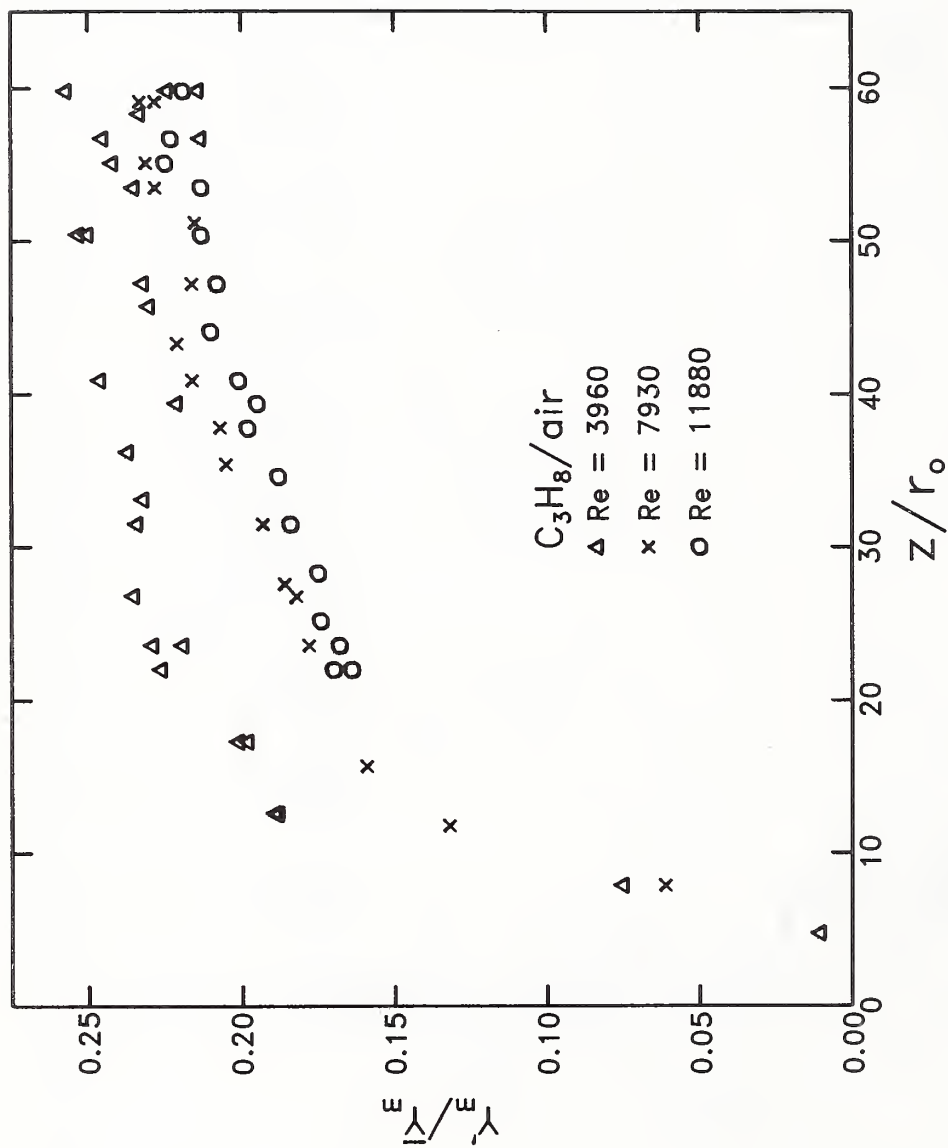Figure 17. The centerline unmixedness values shown in figure 16 are replotted as a function of z/r_ϵ.

Figure 18. Centerline unmixedness values for three different Re jets of propane entering slow coflows of air are plotted as functions of z/r_o.
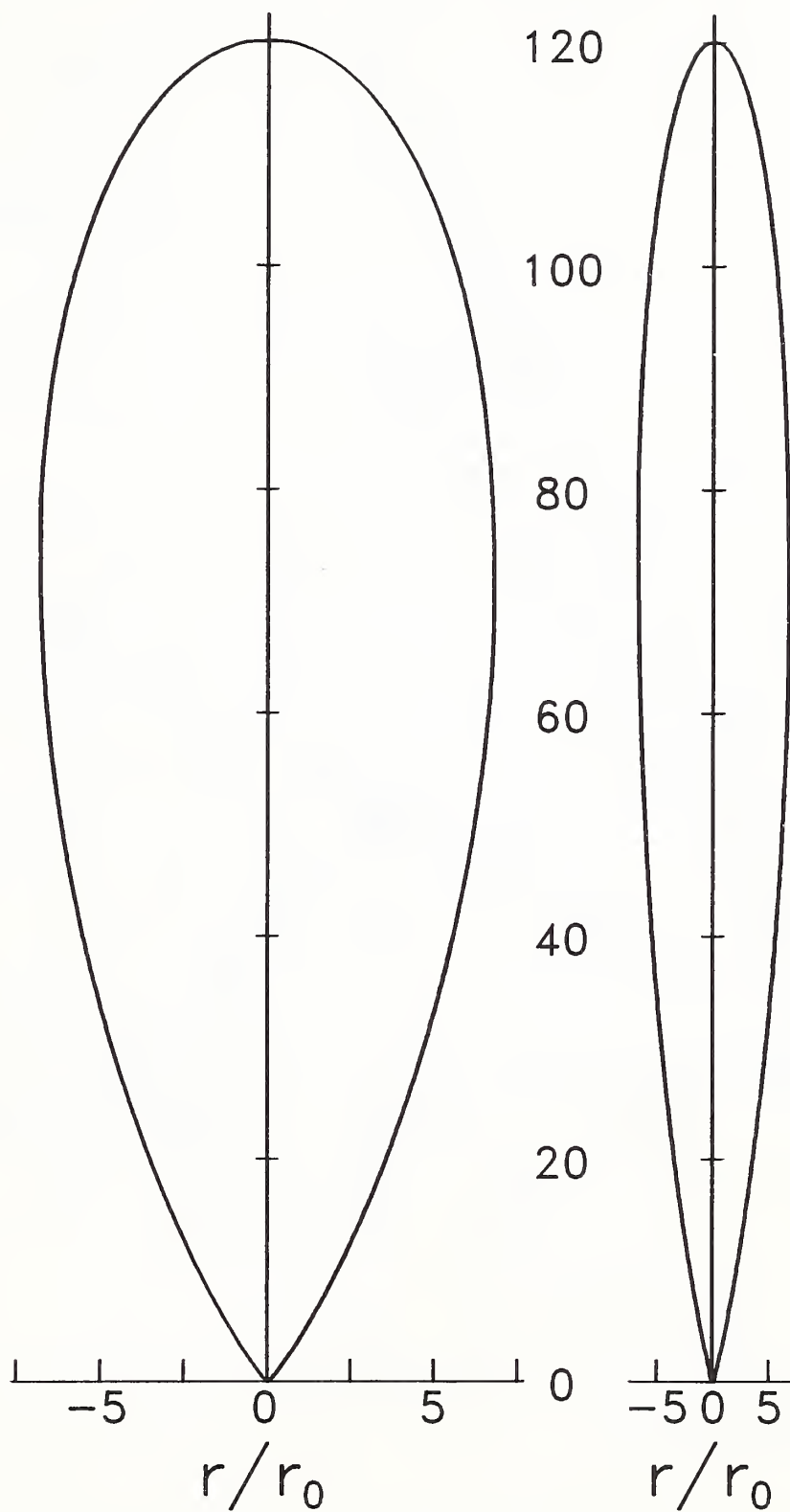
Figure 19. The concentration contour for which the laminar flame speed of an ethylene/air mixture is a maximum.
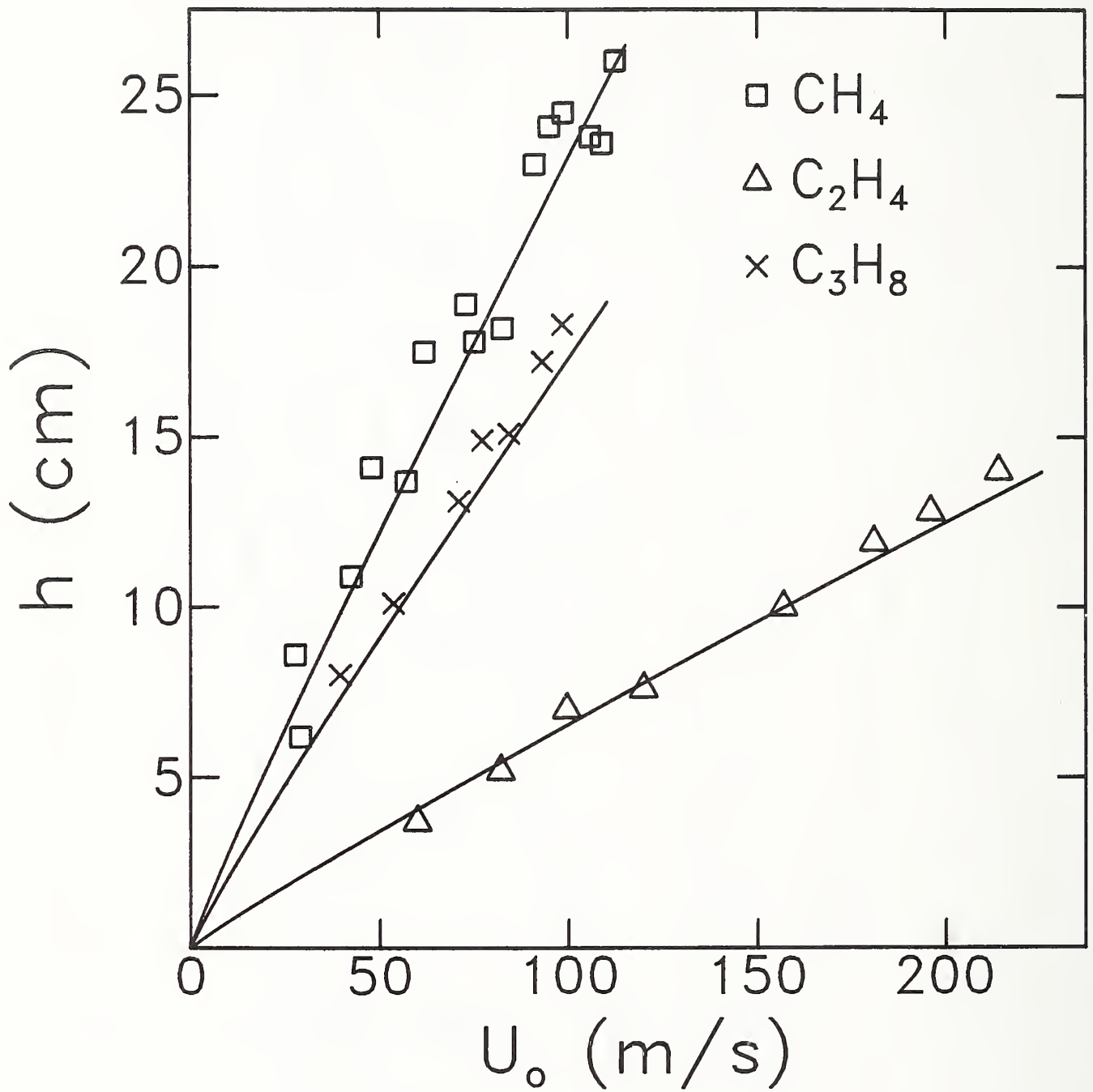
Figure 20.   Experimental values of lift-off height (h) are plotted against jet exit velocity.
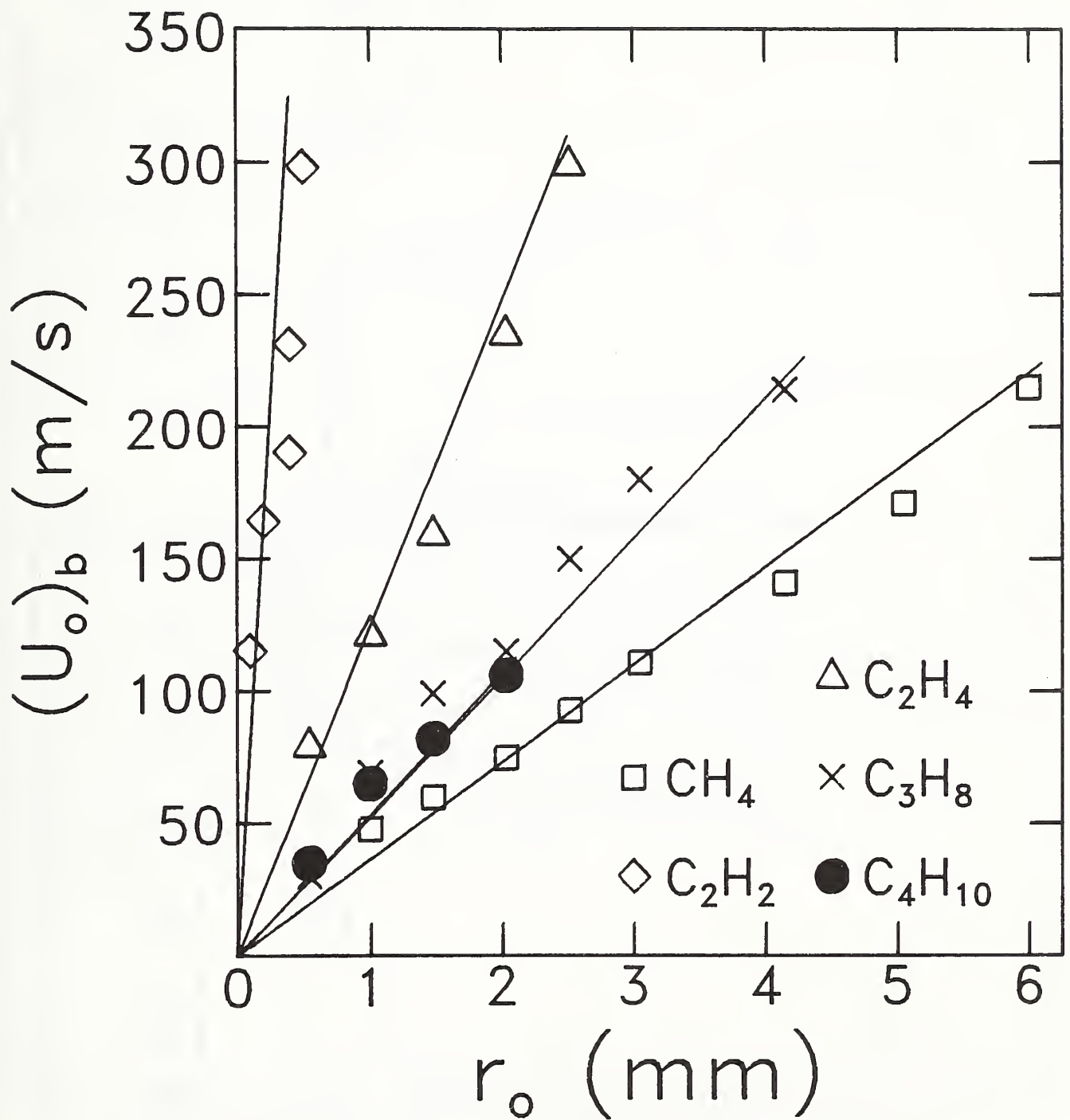
Figure 21. Experimental [53] (symbols) and calculated values (lines) of blow
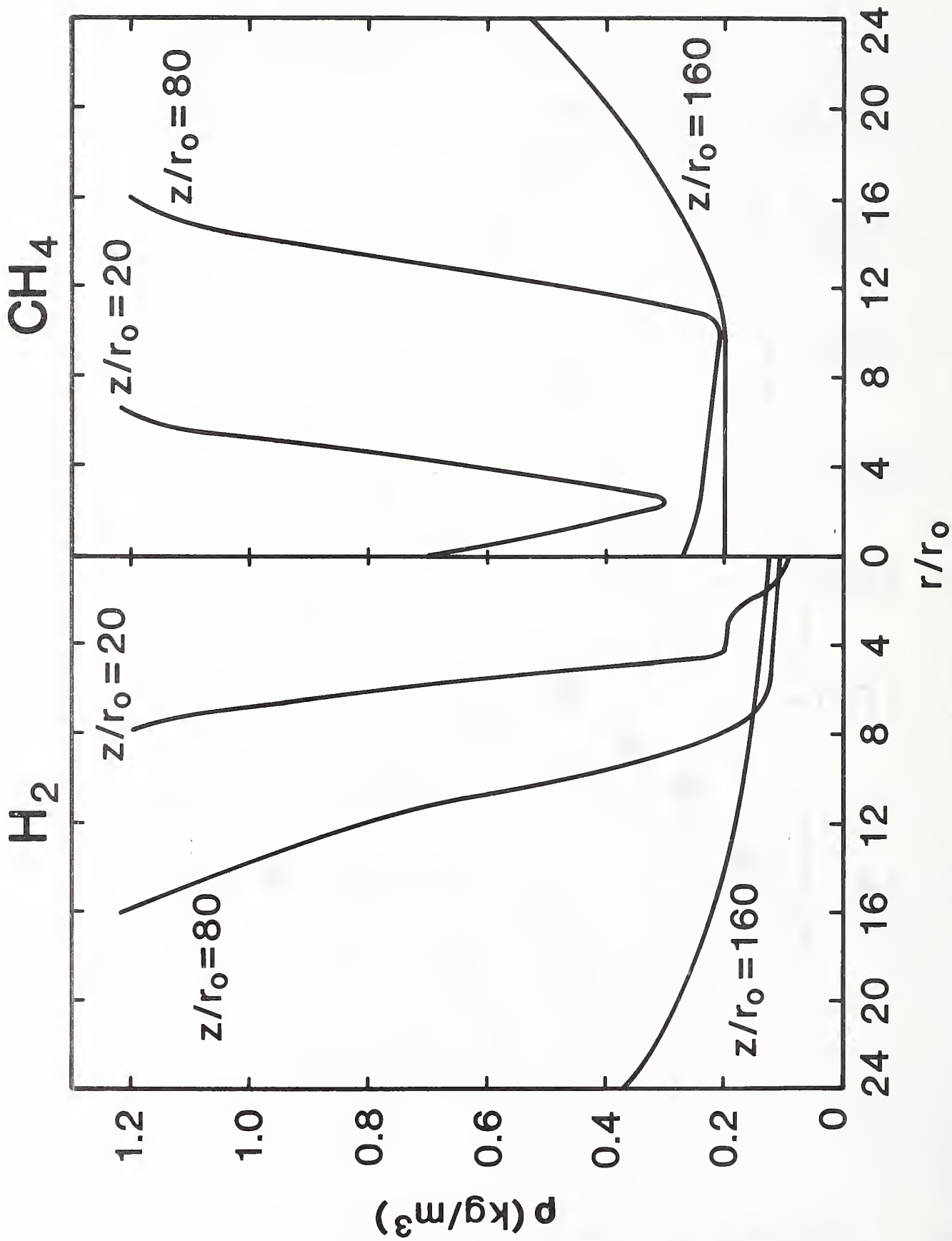out velocity are plotted.

Figure 22. Approximate radial profiles for three nondimensional downstream distances are shown for turbulent jet diffusion flames of hydrogen and a typical organic fuel (methane).

U.S. DEPT. OF COMM. **BIBLIOGRAPHIC DATA** **SHEET** (See instructions)	**1. PUBLICATION OR REPORT NO.** NBSIR-87/3550	**2. Performing Organ. Report No.**	**3. Publication Date** JUNE 1987

4. TITLE AND SUBTITLE

Mixing in Variable Density, Isothermal Turbulent Flow and Implications for Chemically Reacting Turbulent Flows

5. AUTHOR(S)

William M. Pitts and Takashi Kashiwagi

6. PERFORMING ORGANIZATION (If joint or other than NBS, see instructions) **NATIONAL BUREAU OF STANDARDS** **DEPARTMENT OF COMMERCE** **WASHINGTON, D.C. 20234**	**7. Contract/Grant No.** ISSA-86-00008
	8. Type of Report & Period Covered

9. SPONSORING ORGANIZATION NAME AND COMPLETE ADDRESS (Street, City, State, ZIP)

Air Force Office of Scientific Research
Bolling AFB
Building 410
Washington, DC 20332

10. SUPPLEMENTARY NOTES

☐ Document describes a computer program; SF-185, FIPS Software Summary, is attached.

11. ABSTRACT (A 200-word or less factual summary of most significant information. If document includes a significant bibliography or literature survey, mention it here)

This report summarizes the research findings of a project which has been jointly funded by the Air Force Office of Scientific Research and the National Bureau of Standards. The goal of the research was to improve the fundamental understanding of chemically reacting turbulent flow. The approach which was taken was to investigate mixing in variable density flows in order to better understand the role of local density fluctuations (which result from chemical heat release) on the turbulent mixing behavior. The development of new experimental diagnostics having excellent spatial and temporal resolution is described. These techniques have been utilized to investigate a wide range of mixing properties in variable density flows. These results are summarized along with a discussion of their importance to an improved understanding of chemically reacting flow.

12. KEY WORDS (Six to twelve entries; alphabetical order; capitalize only proper names; and separate key words by semicolons)

concentration fluctuations; concentration measurement; density effects; digital line camer; flow visualization; hot wire anemometry; jet flames; Rayleigh light scattering; Reynolds number; turbulent flames; velocity measurement

13. AVAILABILITY [X] Unlimited ☐ For Official Distribution. Do Not Release to NTIS ☐ Order From Superintendent of Documents, U.S. Government Printing Office, Washington, D.C. 20402. [X] Order From National Technical Information Service (NTIS), Springfield, VA. 22161	**14. NO. OF PRINTED PAGES** 73
	15. Price $13.95